

**THE ROLE OF TRYPSIN AND BILE ACIDS IN
ACUTE AND CHRONIC PANCREATITIS**

Ph.D. Thesis

Béla Ózsvári

**First Department of Medicine
University of Szeged**

2008

CONTENTS

ABBREVIATIONS	2
LIST OF FULL PAPERS CITED IN THE THESIS	3
LIST OF ABSTRACTS CITED IN THE THESIS	3
SUMMARY	5
1. INTRODUCTION	7
1.1 THE ROLE OF TRYPSINOGEN AND CHYMOTRYPSINOGEN IN ACUTE PANCREATITIS	7
1.2 THE EFFECTS OF BILE ACIDS AND TRYPSIN ON PANCREATIC DUCTAL EPITHELIUM.....	10
2. MATERIALS AND METHODS	11
2.1 MATERIALS.....	11
2.2 METHODS	12
2.2.1 PURIFICATION OF TRYPSINOGEN.	12
2.2.2. MS/MS PEPTIDE SEQUENCING OF PURIFIED GUINEA PIG TRYPSINOGEN.....	12
2.2.3. COMPLEMENTARY DNA CLONING.	13
2.2.4. ASSAY OF TRYPSIN ACTIVITY.	14
2.2.5. STUDY POPULATION.....	14
2.2.6. MUTATION SCREENING.	15
2.2.7. PLASMID CONSTRUCTION AND MUTAGENESIS.	15
2.2.8. TRANSFECTION OF HUMAN EMBRYONIC KIDNEY 293T AND AR42J CELLS.....	15
2.2.9. CHYMOTRYPSIN C ACTIVITY ASSAY.....	16
2.2.10. PROTEIN BLOTTING.	16
2.2.11. ISOLATION AND CULTURE OF DUCTS.	16
2.2.12. MICROPERFUSION OF PANCREATIC DUCTS.	16
2.2.13. MEASUREMENT OF INTRACELLULAR CALCIUM.	17
2.2.14. IMMUNOHISTOCHEMISTRY.	17
2.2.15. ETHICS.	18
2.2.16. STATISTICS.	18
2.2.17. ACCESSION CODES.	18
3. RESULTS	18
3.1. PURIFICATION OF GUINEA PIG TRYPSINOGENS.....	18
3.2. MS/MS PEPTIDE SEQUENCING OF PURIFIED GUINEA PIG TRYPSINOGEN.....	20
3.3. COMPLEMENTARY DNA CLONING OF GUINEA PIG TRYPSINOGENS.....	20
3.4. ACTIVATION OF GUINEA PIG TRYPSINOGEN.....	23
3.5. CATALYTIC ACTIVITY AND AUTOLYSIS OF GUINEA PIG TRYPSIN.....	24
3.6. DNA SEQUENCING OF THE HUMAN CHYMOTRYPSIN C GENE.....	25
3.7. EXAMINATION OF THE EFFECTS OF PANCREATITIS ASSOCIATED CTRC VARIANTS ON THE SECRETION OF CHYMOTRYPSINOGEN C.	28
3.8. MOLECULAR MODELING OF THE CTRC MUTATIONS.....	31
3.9. EFFECT OF TRYPSIN AND BILE ACIDS ON THE CALCIUM SIGNALLING OF PANCREATIC DUCT EPITHELIAL CELLS.	32
4. DISCUSSION	38
5. ACKNOWLEDGEMENTS	43
6. REFERENCES	44
7. ANNEX	51

ABBREVIATIONS

BAPTA-AM	-	1,2-bis-(o-Aminophenoxy) ethane-N,N,N',N'-tetracetic acid tetra-acetoxymethyl ester
cDNA	-	complementary deoxyribonucleic acid
CTRC	-	chymotrypsin C
Del	-	deletion
DMEM	-	Dulbecco's modified Eagle's medium
DMSO	-	dimethyl sulfoxide
EDTA	-	ethylene diamine tetracetic acid
FBS	-	foetal bovine serum
FURA 2-AM	-	5-Oxazolecarboxylic acid, 2-(6-(bis(carboxymethyl)amino)-5-(2-(2 (bis(carboxymethyl)amino)-5-methylphenoxy)ethoxy)-2-benzofuranyl)-5-oxazolecarboxylic acetoxymethyl ester
HEK	-	human embryonic kidney
HP	-	hereditary pancreatitis
mRNA	-	messenger ribonucleic acid
MS/MS	-	tandem mass spectrometry
PAR-2	-	protease-activated receptor-2
PCR	-	polymerase chain reaction
PRSS1	-	cationic trypsinogen (regular / bold letters – protein / gene)
PRSS2	-	anionic trypsinogen (regular / bold letters – protein / gene)
ROI	-	region of interest
SDS-PAGE	-	sodium dodecyl sulfate polyacrylamide gel electrophoresis
SERCA	-	sarcoplasmic reticulum Ca ²⁺ -ATPase
SMART RACE	-	<u>S</u> witching <u>M</u> echanism <u>A</u> t 5' end of <u>R</u> NA <u>T</u> ranscript, rapid amplification of cDNA ends
SPINK1	-	pancreatic secretory trypsin inhibitor

LIST OF FULL PAPERS CITED IN THE THESIS

1) **Ózsvári B**, Sahin-Tóth M, Hegyi P. The guinea pig pancreas secretes a single trypsinogen isoform, which is defective in autoactivation. *Pancreas* (accepted)

Impact factor: 2.12

2) Rosendahl J, Witt H, Szmola R, Bhatia E, **Ózsvári B**, Landt O, Schulz HU, Gress TM, Pfützer R, Löhr M, Kovacs P, Blüher M, Stumvoll M, Choudhuri G, Hegyi P, Morsche RHM, Drenth JPH, Truninger K, Macek M Jr, Puhl G, Witt U, Schmidt H, Buning C, Ockenga J, Kage A, Groneberg DA, Nickel R, Berg T, Wiedenmann B, Bodeker H, Keim V, Mossner J, Teich N, Sahin-Tóth M. Chymotrypsin C (CTRC) alterations that diminish activity or secretion are associated with chronic pancreatitis. *Nature Genetics* 2008; 40:78-82.

Impact factor: 24.18

3) Venglovecz V, Rakonczay Z Jr, **Ózsvári B**, Takács T, Lonovics J, Varró A, Gray MA, Argent BE, Hegyi P. Differential effects of bile acids on pancreatic ductal bicarbonate secretion in guinea pig. *Gut* (under final revision)

Impact factor: 9.002

LIST OF ABSTRACTS CITED IN THE THESIS

4) Hegyi P, **Ózsvári B**, Ignáth I, Venglovecz V, Rakonczay Z Jr, Takács T, Borka K, Schaff Zs, Papp Gy J, Tóth A, Varró A, Sahin-Tóth M, Lonovics J. The effects of trypsin on pancreatic PAR-2 receptors. *Pancreas*, 2006; 33: 468-469

5) Ignáth I, **Ózsvári B**, Venglovecz V, Rakonczay Z Jr, Takács T, Lonovics J, Borka K, Schaf Z, Tóth A, Varró A, Sahin-Tóth M, Hegyi P. Localization and functional characterization of PAR-2 receptor in guinea pig pancreatic duct cells. *Pancreatology*, 2006; 6:326

LIST OF FULL PAPERS RELATED TO THE SUBJECT OF THE THESIS

6) Tóth-Molnár E, Venglovecz V, **Ózsvári B**, Rakonczay Z Jr., Varró A, Tóth A, Lonovics J, Takács T, Ignáth I, Iványi B, Hegyi P. A New Experimental Method to Study the Acid/Base Transporters and their Regulation in Lacrimal Gland Ductal Epithelia. *Invest Ophthal Vis Sci*, 2007;48:3746-55.

Impact factor: 3.64

7) Hegyi P, Rakonczay Z, Farkas K, Venglovecz V, **Ózsvári B**, Seidler U, Gray MA, Argent BE. Controversies in the role of SLC26 anion exchangers in pancreatic ductal bicarbonate secretion. *Pancreas*, 07-00649, (accepted)

Impact factor: 2.12

Number of full publications:	4
Cumulative impact factor:	41.06
Number of abstract publications:	15
Number of scientific presentations:	22

SUMMARY

Background. Acute pancreatitis usually develops due to the blockage of the main pancreatic duct by a gallstone, whereas chronic pancreatitis is a series of recurring inflammatory attacks, where the primary cause is mostly alcoholism. Hereditary chronic pancreatitis is a rare form of early onset chronic pancreatitis, which accumulates in selected families suggesting a genetic background. These pancreatic diseases show variable severity in which some patients manifest a severe, highly morbid, and frequently lethal attack during acute inflammation, while others experience mild, self-limited attacks mostly during chronic inflammation. It is generally believed that the earliest events in acute pancreatitis occur within acinar cells and the digestive protease trypsin plays a fundamental pathogenetic role in the initiation of cell injury, however, the exact intraacinar mechanisms by which diverse etiological factors induce an attack are still unclear.

The **aims** of the present investigations summarized in this thesis were to examine the role of trypsin and bile acids in the initiation of acute and chronic pancreatitis. We purified and cloned the trypsinogen isoforms from the guinea pig pancreas and characterized their activation properties. We analyzed the gene encoding the trypsin-degrading enzyme chymotrypsin C (*CTRC*) in German subjects with idiopathic or hereditary chronic pancreatitis and determined the activity and/or secretion abnormalities of the most frequent variants. Thirdly, we characterised the effect of trypsin and bile acids on the intracellular calcium signalling of guinea pig pancreatic duct epithelial cells.

Methods. Guinea pig trypsinogens from pancreatic homogenates were isolated by ecotin-affinity chromatography, followed by cation-exchange chromatography. Complementary DNAs for pre-trypsinogens were cloned from total RNA after reverse transcription and PCR-amplification, activation of trypsinogens was tested with enteropeptidase, cathepsin B and trypsin.

We carried out direct DNA sequencing of the *CTRC* gene in 2804 control and 901 affected individuals with chronic pancreatitis. Then, plasmids carrying the wild-type and the most frequent variants of *CTRC* were constructed by overlap extension PCR mutagenesis. The plasmids were expressed in human embryonic kidney (HEK) cells and AR42J rat pancreatic acinar cells through transient transfection. Chymotrypsin C activity assay and protein blotting were performed from the media and cell extract of the transfected samples to determine possible secretion and/or activity changes of the variants.

Pancreatic ducts were isolated from guinea pig, after overnight culture at 37 °C, then the ducts were loaded with the calcium sensitive fluorescent dye FURA-2. Intracellular calcium measurements were performed using the Cell^R Imaging System.

Results and discussion. Purification of trypsinogens yielded a single peak with an N-terminal amino-acid sequence of LPIDD. Cloning of pre-trypsinogen cDNAs revealed two distinct but nearly identical isoforms. At the amino acid level, the only difference between the two isoforms is an Ala/Ser change at position 15 within the signal peptide. Thus, both cDNA variants give rise to the same mature trypsinogen upon secretion. Guinea pig trypsinogen is readily activated by enteropeptidase and cathepsin B, but exhibits essentially no autoactivation, under conditions where human cationic and anionic trypsinogens rapidly autoactivate. The observations suggest that multiple trypsinogen isoforms and their ability to autoactivate are not required universally for normal digestive physiology in mammals. Furthermore, the inability of guinea pig trypsinogen to undergo autoactivation suggests that this species might be more resistant to pancreatitis than humans, where increased autoactivation of cationic trypsinogen mutants has been linked to hereditary pancreatitis.

During the mutation screening of the chymotrypsin C gene, we found two alterations, p.R254W (arginine > tryptophan) and p.K247_R254del (deletion of 8 amino acids), which were significantly over-represented in the pancreatitis group and were present in 30/901 (3.3%) affected individuals but only in 21/2,804 (0.7%) controls. A replication study identified these two variants in 10/348 (2.9%) individuals with alcoholic chronic pancreatitis but only in 3/432 (0.7%) subjects with alcoholic liver disease. Chymotrypsin C variants were also found in 10/71 (14.1%) Indian subjects with tropical pancreatitis but only in 1/84 (1.2%) control. Functional analysis of the chymotrypsin C variants revealed impaired activity and/or reduced secretion. The results indicate that loss-of-function alterations in chymotrypsin C predispose to pancreatitis by diminishing its protective trypsin-degrading activity. In summary, the genetic and functional data of our study identifies chymotrypsin C as a new pancreatitis-associated gene.

Experiments on the effects of trypsin on guinea pig pancreatic ducts showed that trypsin dose-dependently activated Ca²⁺-signalling from the basolateral membrane of the cells and the protease-activated receptor-2 (PAR-2) agonist mimicked the effect. Soybean trypsin inhibitor and the calcium chelator BAPTA-AM totally blocked the basolateral effect of trypsin on intracellular calcium concentration ([Ca²⁺]_i). Trypsin also evoked Ca²⁺ signalling in a Ca²⁺ free external solution, suggesting that Ca²⁺ is presumably released from intracellular stores. Luminal administration of trypsin also elevated [Ca²⁺]_i suggesting

the luminal localization of the PAR-2. Immunohistochemical analyses confirmed that the PAR-2 is expressed on the luminal membrane of intralobular but not interlobular ducts.

Examinations on the effects of bile acids on primary pancreatic ducts revealed that both basolateral and luminal administration of high doses of chenodeoxycholate and glycochenodeoxycholate triggered calcium responses in guinea pig pancreatic duct epithelial cells, while only the low dose of chenodeoxycholate and not glycochenodeoxycholate caused calcium signals in the cells. Neither the parasympatholytic atropine nor removal of calcium from the extracellular standard HEPES solution had any effect on the elevation of $[Ca^{2+}]_i$ evoked by luminal administration of low dose of chenodeoxycholate. However, the calcium-chelator, BAPTA-AM, and the inositol triphosphate (IP_3) receptor inhibitor caffeine totally blocked the calcium response. Both the IP_3 receptor inhibitor xestospongine C and the phospholipase C inhibitor U73122 blocked the intracellular calcium response of low doses of chenodeoxycholate and slightly inhibited the $[Ca^{2+}]_i$ elevation of high doses of chenodeoxycholate of basolateral and luminal administration.

These experiments on the effects of trypsin and bile acids on pancreatic ducts suggests that PAR-2 may be the target by which pancreatic duct cells are activated by trypsin at the early stages of acute pancreatitis. During pathological conditions, when a bile stone impacts in the ampulla of Vater resulting in bile reflux into the pancreatic ductal system, bile acids can also activate pancreatic ductal epithelial cells through intracellular calcium signalling mechanisms and the activated cells might play an important role during the inflammation of pancreatic tissue.

1. INTRODUCTION

1.1 The role of trypsinogen and chymotrypsinogen in acute pancreatitis

Trypsinogen is the most abundant digestive protease of the pancreas which, under normal conditions, becomes active only when it is secreted into the duodenum. However, numerous studies have concluded that premature activation of intraacinar trypsinogen is a critical initiating factor that leads to the injury of acini, cell death and finally to acute pancreatitis [1].

The human pancreas secretes three isoforms of trypsinogen, encoded by the protease, serine (*PRSS*) genes 1, 2 and 3. On the basis of their relative electrophoretic mobility, the three trypsinogen species are commonly referred to as cationic trypsinogen (product of *PRSS1*), anionic trypsinogen (product of *PRSS2*), and mesotrypsinogen (product of *PRSS3*) [2]. While individual variations definitely exist, normally the cationic isoform constitutes about 2/3 of the total trypsinogen content, and anionic trypsinogen makes up approximately 1/3 [3, 4, 5]. Mesotrypsinogen is a minor species, accounting for less than 5% of trypsinogens in human pancreatic juice [6, 7]. Human trypsinogens are synthesized as proenzymes with 247 amino acid containing a signal peptide of 15 residues, followed by the above mentioned trypsinogen activation peptide. The signal peptide is removed upon entry into the endoplasmic reticulum lumen and the proenzymes (also called zymogens) are packed into zymogen granules and eventually secreted into the pancreatic juice. The intestinal endopeptidase, enterokinase, produced by enterocytes [8], converts trypsinogen to trypsin by release of the N-terminal octapeptide (trypsinogen activation peptide).

Chymotrypsinogen is the second proenzyme in the cascade of pancreatic protease activation and can be activated by trypsin [9]. The striking similarity between chymotrypsinogen and trypsinogen is well known, they have highly homologous primary and tertiary structures [10], such as the number and composition of amino acids. The main difference between the two enzymes lies in their substrate specificity. While trypsin hydrolyses the polypeptide chain at the lysyl and arginyl bonds, chymotrypsin selectively cleaves peptide bonds formed by aromatic residues, like phenylalanine, tyrosine and tryptophan [11, 12]. The major chymotrypsin isoform in the human pancreas is chymotrypsin B, which is expressed as two nearly identical isoforms (CTRB1 and CTRB2) [13], the third minor isoform is chymotrypsin C. Chymotrypsin C was first isolated from pig pancreas and was shown to exhibit protease activity distinct from the bovine or porcine chymotrypsin A or the bovine chymotrypsin B [14]. Recently, chymotrypsin C-mediated acceleration of trypsinogen activation has been described and compared to the autoactivation of chymotrypsin C-cleaved normal cationic trypsinogen, the pancreatitis-associated mutation A16V in cationic trypsinogen increased the rate of autoactivation *in vitro*. Thus, the chymotrypsin C-mediated stimulation of autoactivation plays a role in the pathogenesis of human pancreatitis [15]. Novel findings show that chymotrypsin C has been identified as a key regulator of activation and degradation of cationic trypsin. Thus, in the high Ca^{2+} environment of the duodenum, chymotrypsin C facilitates trypsinogen

activation, whereas in the lower intestines, chymotrypsin C promotes trypsin degradation as a function of decreasing luminal Ca^{2+} concentrations [16].

At present, it is widely accepted that the premature activation of digestive enzymes within the pancreatic acinar cells is a critical initiating event leading to autodigestion of pancreas [17, 18, 19, 20]. Inappropriate activation of trypsinogen can take place in the zymogen granules of acinar cells [21] but the exact process of activation is still controversial. There are several hypotheses of intra-acinar trypsinogen activation. According to the trypsinogen autoactivation theory, trypsin-induced trypsinogen activation or autoactivation is the triggering event that occurs in the acini [22]. The colocalization hypothesis describes that the lysosomal cysteine protease cathepsin B plays an essential role in the mechanisms of trypsinogen activation as cathepsin B during the inappropriate colocalization of lysosomes with zymogen granules may activate trypsinogen, as it was proved in *in vitro* studies [23, 24]. Prolonged high concentration of calcium in acinar cells might also be an important initial factor in disrupted cell signalling that leads to cellular injury. Pancreatic secretory trypsin inhibitor, or in other words, serine protease inhibitor, Kazal type I (SPINK1) is also present in secretory granules of acinar cells that is thought to be a specific inactivation factor of intrapancreatic trypsin activity. Defect of this inhibitor can result in the imbalance of trypsinogen activation and trypsin inactivation that leads to pathological conditions. When more than about 10-20% of trypsinogen is activated intracellularly, the inhibitory mechanism is no longer effective, cellular injury occurs, which leads to the death of acinar cells and finally to acute pancreatitis [25, 26].

Comfort and Steinberg were first to recognize that chronic pancreatitis may accumulate in selected families suggesting a genetic background [27]. Thereafter, hereditary chronic pancreatitis was defined as an autosomal dominant disease with a penetrance of approximately 80%. In the past decade, intense research has been performed to identify mutations in trypsinogen genes that could be associated with pancreatitis. To date, 22 *PRSSI* gene variants have been found, which are, interestingly, located in the N-terminal part of the protein. The three most prevalent mutations according to frequency of occurrence are R122H (approximately 70%), N29I (approximately 25%), and A16V (approximately 4%). The R122H mutation was the first identified cationic trypsinogen variant [28]. It shows increased trypsinogen autoactivation and also increased trypsin stability because the mutation decreases autolysis as Arg122 is an important autolytic site. The N29I was found to have normal autolysis but enhanced autoactivation, which led to the conclusion that increased autoactivation is the common pathogenic mechanism of

hereditary pancreatitis-associated PRSS1 mutations [29]. The third most frequent variant, A16V, which alters the N-terminal amino acid of trypsinogen, has appeared to be an exception, as in a recent study, the A16V mutant failed to exhibit increased autoactivation [30]. Interestingly, the genetic variants of PRSS2 or PRSS3 have not been described in association with chronic pancreatitis [31, 32], although, a recent paper has proved that a PRSS2 variant, G191R, which was surprisingly over-represented in the control group, results in a degradation-sensitive protein that protect against chronic pancreatitis [33].

1.2 The effects of bile acids and trypsin on pancreatic ductal epithelium

Exposure of the pancreas to bile acids is considered to be one of the possible causes of acute pancreatitis. Since the pancreatic and bile ducts share a common outflow into the duodenum, the obstruction of the ampulla of Vater may cause bile to penetrate into the pancreatic duct, exposing the pancreas to bile acids [34]. Although the bile can reach both acinar and ductal cells during biliary pancreatitis, much more research has been done on acinar cells. Bile acids have been shown to induce Ca^{2+} signalling in pancreatic acinar cells via an IP_3 -dependent mobilization of intracellular Ca^{2+} and an inhibition of SERCA- (Sarcoplasmic Reticulum Ca^{2+} -ATPase) dependent Ca^{2+} reloading into intracellular pools [35]. The elevated intracellular Ca^{2+} concentration can lead to enzyme activation [36] and/or cell death [37], and result in severe acute necrotizing pancreatitis. These data suggest that Ca^{2+} toxicity could be an important factor contributing to bile acid-induced cellular damage in both the acinar and also the ductal epithelial cells.

It has been shown, that retrograde injection of Na-taurocholate into the rat pancreatic duct induces fluid hypersecretion and decreases protein output in the initial phase of acute pancreatitis [38]. We believe that the pancreatic ductal epithelium is at least in part involved in the hypersecretory effect of bile acids, which may represent a defence mechanism against bile acids in order to avoid pancreatic injury. The aim of the third part of the thesis was to characterize the effects of bile acids and trypsin on the intracellular Ca^{2+} signalling of pancreatic duct epithelial cells. We performed our experiments on intact isolated guinea pig pancreatic ducts, because the guinea pig pancreas secretes a juice containing ~140mM NaHCO_3 as does the human gland [39].

Protease-activated receptors (PARs) are a family of G-protein coupled receptors activated by proteolysis [40]. Specific serine proteases cleave the extracellular portion of

the receptor protein to generate a tethered ligand. This tethered ligand activates the receptor triggering intracellular signalling. PAR-2 is specifically activated by trypsin and is localized along the pancreatic ductal systems as well as the gastrointestinal tract, kidney, liver, bronchial tree, prostate, ovary, brain and eye [41]. Furthermore, PAR-2 receptor has been identified in acinar cells and linked to the release of amylase [42]. Nguyen et al. detected PAR-2 in dog pancreatic duct cells and found that the activation of PAR-2 led to increased Ca^{2+} -activated Cl^- and K^+ conductances, linking the activation of the receptor with pancreatic secretory function [43]. They localized the receptor to the basolateral membrane by immunofluorescent staining of the tissue. Alvarez et al. described the presence of PAR-2 in bovine main pancreatic ducts but they revealed the inhibitory effects of trypsin on bicarbonate secretion and localized the receptor to the apical membrane [44]. Detection of PAR-2 in human pancreatic ductal adenocarcinoma cells has been described by immunoblotting [45]. These controversial studies have led us to examine the function of PAR-2 receptors in guinea pig pancreatic ducts.

2. MATERIALS AND METHODS

2.1 MATERIALS

Whole pancreata from Abyssinian guinea pigs were purchased from Rockland Immunochemicals (Gilbertsville, PA). The pancreata were flash frozen in liquid nitrogen, shipped on dry ice and stored at $-80\text{ }^\circ\text{C}$. RNAqueousTM Phenol-free total RNA Isolation kit was from Ambion Inc. (Austin, TX, USA), SMARTTM RACE cDNA Amplification Kit from Clontech Laboratories Inc. (Mountain View, CA), Zero Blunt TOPO PCR Cloning Kit from Invitrogen Corp. (Carlsbad, CA, USA) and *N*-CBZ-Gly-Pro-Arg-*p*-nitroanilide from Sigma-Aldrich (St. Louis, MO, USA). Recombinant human pro-enteropeptidase was from R&D Systems (Minneapolis, MN, USA). Human recombinant cathepsin B was a generous gift from Paul M. Steed (Research Department, Novartis Pharmaceuticals, Summit, New Jersey, USA).

The compositions of the solutions used for measurements of intracellular calcium concentration are shown in Table 1. Chromatographically pure collagenase was purchased from Worthington (Lakewood, NJ, USA). CellTak was obtained from Becton Dickinson Labware (Bedford, MA, USA). 2-(6-(bis(carboxymethyl)amino)-5-(2-(2-(bis(carboxymethyl)amino)-5-methylphenoxy)ethoxy)-2-benzofuranyl)-5-

oxazolecarboxylic acetoxymethyl ester (FURA 2-AM), and 1,2-bis(o-aminophenoxy)ethane-N,N,N',N'-tetraacetic acid (BAPTA-AM) were from Molecular Probes Inc. (Eugene, OR, USA). Coomassie Brilliant Blue R-250 was from Pierce Biotechnology, Inc. (Rockford, IL, USA) Trypsin, bile acids and all other chemicals were obtained from Sigma-Aldrich (Budapest, Hungary). BAPTA-AM was dissolved in dimethyl sulfoxide (DMSO), FURA 2-AM in DMSO containing 20 % pluronic acid.

	Standard HEPES	Standard HCO₃⁻	Ca²⁺-free HEPES
NaCl	130	115	132
KCl	5	5	5
MgCl₂	1	1	1
CaCl₂	1	1	
Na-HEPES	10		10
Glucose	10	10	10
NaHCO₃		10	

Values are concentrations in mM.

Table 1. Composition of solutions used for measurements of intracellular calcium concentration.

2.2 METHODS

2.2.1 Purification of trypsinogen. Guinea pig pancreatic tissue (5 g) was homogenized in 0.1 M Tris-HCl, pH 8.0 using a rotor-stator tissue homogenizer (T 25, IKA Works, USA) at 11,000 – 13,000 rpm and the homogenate was centrifuged for 8 min at 13,000 rpm, at 4 °C. The supernatant was further clarified by a second round of centrifugation, and then loaded onto a 2 mL ecotin-affinity column [46]. The column was washed with 20 mM Tris-HCl (pH 8.0), 0.2 M NaCl and elution was performed with 50 mM HCl. The ecotin-eluate (~1 mg protein in 3-4 mL volume) was directly loaded onto a Mono S HR 5/5 strong cation-exchange column equilibrated with 20 mM Na-acetate (pH 5.0). The Mono S column was developed with a linear gradient of 0-0.5 M NaCl. Concentrations of guinea pig trypsinogen preparations were estimated from UV absorbance at 280 nm, using a theoretical extinction coefficient of 37,650 M⁻¹ cm⁻¹ (<http://ca.expasy.org/tools/protparam.html>).

2.2.2. MS/MS peptide sequencing of purified guinea pig trypsinogen. To obtain independent sequence information from the purified guinea pig trypsinogen, a sample was subjected to tandem MS (mass spectrometric) peptide sequencing by ProtTech Inc,

Eagleville, PA, USA. After electrophoresis on a 15 % SDS-PAGE, the trypsinogen band was excised and digested in-gel with sequencing grade modified porcine trypsin (Promega Corp, Madison, WI, USA). The resulting mixture was then analyzed by LC (liquid chromatography)-MS/MS (ProtTech, Inc, Eagleville, PA, USA).

2.2.3. Complementary DNA cloning. Total RNA isolation was performed from 30 mg homogenized guinea pig pancreas by the RNAqueous™ kit. Phenol-free total RNA Isolation kit modified with an additional phenol-chloroform extraction. First-strand cDNA was synthesized using the SMART™ RACE cDNA Amplification Kit with 2 µg RNA. For the 5' RACE reaction, first-strand synthesis was primed with an oligo(dT) primer. The reverse transcriptase used in the reaction exhibits terminal transferase activity and adds a series of dC residues to the 3' end of the cDNA. An oligonucleotide (SMART IIA) present in the reaction mixture anneals to the dC stretch and serves as template for further extension of the cDNA. The end result of the reaction is a full length cDNA with an additional SMART sequence at the 5' end. For the 3' RACE, the mRNA is reverse transcribed with an oligo(dT) primer which anneals to the polyA tail and also incorporates the SMART sequence at its 5' end. Guinea pig trypsinogen cDNA was PCR-amplified in 2 reactions from the first-strand 5' and 3' RACE cDNAs using a gene-specific primer and a Universal primer that annealed against the SMART sequence incorporated into the first-strand cDNA either at the 5' or 3' ends. The gene specific GP1 primers annealed with relatively low stringency to the region around the conserved catalytic Ser200 (see Fig 2); the GP1 sense primer (5`-TGT CAG GGA GAC TCT GGT GGC CCA GTT GTC TGC-3`) corresponded to codons 196-206, and the GP1 antisense primer (5`-GCA GAC AAC TGG GCC ACC AGA GTC TCC CTG-3`) corresponded to codons 197-206 (Fig 2). These primers were previously designed against the corresponding region of the *Bothrops jararaca* trypsinogen (GenBank #AF190273) and used successfully in other cloning projects in our laboratory. PCR products were purified and directly subcloned into the pCR-Blunt II-TOPO vector using the Zero Blunt TOPO PCR Cloning Kit (Invitrogen). Fifteen clones from the 5' RACE reaction and 3 clones from the 3' RACE reaction were sequenced. The initial sequence information indicated that 2 almost identical cDNA species were cloned. On the basis of the initial sequencing results, new trypsinogen-specific primers were designed. The GP2 sense primer (5'- AGC TAC AGC AGC AGC ACC CTG AAC -3') anneals to codons 98-105, and the GP2 antisense primer (5'- GAT CTG TCC AGG ATA GGC GGA CTG -3') anneals to codons 172-179 (Fig 2). Using the GP2 primers and the Universal primer additional trypsinogen-specific amplicons were

generated from the first-strand 5' RACE and 3' RACE cDNA and subcloned into the pCR-Blunt II-TOPO vector. Five clones from the 5' RACE reaction and 4 clones from the 3' RACE reaction were sequenced. Finally, the full length cDNA sequences of the 2 guinea pig pre-trypsinogen isoforms were reconstructed from overlapping fragments. The guinea pig pre-trypsinogen cDNA sequences have been deposited to GenBank under accession numbers EF371801 and EF371802.

2.2.4. Assay of trypsin activity. Trypsin activity was determined using the synthetic chromogenic substrate *N*-CBZ-Gly-Pro-Arg-*p*-nitroanilide. Kinetics of the chromophore release was followed at 405 nm in 0.1 M Tris-HCl (pH 8.0), 1 mM CaCl₂, at 22 °C using a Spectramax Plus 384 microplate reader (Molecular Devices Corp., Sunnyvale, CA, USA).

Human trypsinogens were expressed in *Escherichia coli* and affinity-purified as described previously [47, 29, 48, 49]. Human pro-enteropeptidase (0.07 mg/mL stock solution) was activated with 50 nM human cationic trypsin in 0.1 M Tris-HCl (pH 8.0), 10 mM CaCl₂ and 2 mg/ml bovine serum albumin (final concentrations) for 30 min at room temperature. Before use, cathepsin B was activated with 1 mM dithiothreitol (final concentration) for 30 min on ice.

2.2.5. Study population. The study (screening of human chymotrypsin C gene) was approved by the medical ethical review committees of the University of Leipzig and the Charité University Hospital. All affected individuals gave informed consent. We enrolled 1,320 unrelated individuals with the diagnoses of hereditary (n = 143) or idiopathic chronic pancreatitis (n=758) or alcoholic chronic pancreatitis (n = 348) and originating from Germany. In addition, we also investigated subjects affected with tropical calcific pancreatitis originating from India (n = 71). The diagnosis of chronic pancreatitis was based on two or more of the following findings: presence of a typical history of recurrent pancreatitis, pancreatic calcifications and/or pancreatic ductal irregularities revealed by endoscopic retrograde pancreaticography or by magnetic resonance imaging of the pancreas, and pathological sonographic findings. Hereditary chronic pancreatitis was diagnosed when one first-degree relative or two or more second-degree relatives suffered from recurrent acute or chronic pancreatitis without apparent precipitating factors. Affected individuals were classified as having idiopathic chronic pancreatitis when precipitating factors, such as alcohol abuse, trauma, medication, infection, metabolic disorders or a positive family history consistent with hereditary pancreatitis, were absent.

Alcohol-induced chronic pancreatitis was diagnosed in patients who consumed more than 60 g (females) or 80 g (males) of ethanol per day for more than 2 years. Control subjects free of pancreatic diseases were recruited from Germany (n = 2,804) and India (n = 81). The German controls included parents of children recruited to the German Multicenter Allergy Study, healthy controls recruited for a genetic study on type 2 diabetes at the University Hospital at Leipzig, blood donors, medical students, and staff and subjects recruited to the Berlin Aging Study. In addition, 432 German subjects with alcoholic liver disease but without pancreatic disease were recruited as controls for the alcoholic chronic pancreatitis group.

2.2.6. Mutation screening. Genomic DNA was extracted from whole blood samples. Oligonucleotide sequences, PCR and cycle sequencing conditions are available in the Annex (see Supplementary methods). Briefly, we digested the PCR products with shrimp alkaline phosphatase and exonuclease I and performed cycle sequencing using BigDye terminator mix (Applied Biosystems). The reaction products were purified with ethanol precipitation or Sephadex G-50 and loaded onto an ABI 3100 or an ABI 3730 sequencer (Applied Biosystems).

2.2.7. Plasmid construction and mutagenesis. We constructed the pcDNA3.1(-)_CTRC (human chymotrypsinogen C) expression plasmid using the IMAGE clone #5221216 (GenBank: BI832476), as described by Szmola R et al. [16]. Chymotrypsinogen C mutants and the Glu-Glu-tagged constructs were generated by overlap extension PCR mutagenesis and ligated into pcDNA3.1(-). The Glu-Glu tag sequence (EYMPME) is derived from the polyoma virus medium T antigen.

2.2.8. Transfection of human embryonic kidney 293T and AR42J cells. Human embryonic kidney (HEK) 293T cells were cultured and transfected as described [50]. Approximately 10⁶ cells per well were plated in six-well tissue culture plates in Dulbecco's Modified Eagle's Medium (DMEM) (Invitrogen) supplemented with 10% fetal bovine serum (FBS) and 4 mM glutamine. We carried out transfections using 4 mg pcDNA3.1(-)-CTRC plasmid (carrying the wild type or the mutant CTRC variants) and 10 ml Lipofectamine 2000 (Invitrogen) in 2 ml OptiMEM medium (Invitrogen) supplemented with 2 mM glutamine. After 5 h incubation at 37 °C, 2 ml DMEM with 20% FBS and 4 mM glutamine was added to each well, and cells were incubated for an additional 24 h. Then we washed the cells with 1 ml OptiMEM and 2 mM glutamine and replaced the transfection medium with 2 ml OptiMEM and 2 mM glutamine. Time courses of

expression were measured starting from this medium change and were followed for 48 h. AR42J cells were maintained as subconfluent cultures in DMEM containing 20% FBS, 4 mM glutamine and 1% penicillin/streptomycin solution. Cells (10^6 /well) were plated into 35-mm wells and grown in the presence of 100 nM dexamethasone for 48 h. We carried out transfections using the Glu-Glu-tagged CTRC constructs, as described above. After 48 h, we replaced the medium with fresh OptiMEM and 2 mM glutamine, and we added 1 nM cerulein (final concentration) to stimulate secretion. After 15 min of incubation, the medium was collected and analyzed by protein blotting.

2.2.9. Chymotrypsin C activity assay. The conditioned medium was supplemented with 0.1 M Tris-HCl (pH 8.0) and 10 mM CaCl_2 (final concentrations) and CTRC was activated with 100 nM human cationic trypsin (final concentration) for 20 min at 37 °C. We measured CTRC activity with Suc-Ala-Ala-Pro-Phe-p-nitroanilide or Glt-Ala-Ala-Pro-Leu-p-nitroanilide (0.15 mM final concentration) in 0.1 M Tris-HCl (pH 8.0), 1 mM CaCl_2 , at room temperature.

2.2.10. Protein blotting. Samples were run on 15% Tris-glycine gels under reducing conditions and transferred onto an Immobilon-P membrane (Millipore) at 300 mA for 1 h. The membrane was blocked with 5% non-fat dry milk overnight and incubated with a horse radish peroxidase-conjugated goat polyclonal antibody against the Glu-Glu tag at a concentration of 0.1 $\mu\text{g}/\text{mL}$ for 1 h at room temperature. Horse radish peroxidase was detected using the SuperSignal West Pico Chemiluminescent Reagent (Pierce, Rockford, IL, USA).

2.2.11. Isolation and culture of ducts. Small intra/interlobular ducts were isolated from the pancreas of guinea pigs weighing 150-250g. The guinea pig was humanly killed by cervical dislocation, the pancreas was removed and intra/interlobular ducts were isolated as described previously [51, 52, 53, 54]. The ducts were cultured overnight in a 37 °C incubator gassed with 5 % CO_2 /95 % air. During the overnight incubation both ends of the isolated ducts seal and the ducts swell due to fluid secretion into the lumen [55].

2.2.12. Microperfusion of pancreatic ducts. The lumen of the cultured ducts was microperfused using a modification of the method described by Ishiguro et al [56]. Briefly, one end of a sealed duct was cut off using a 26G x $\frac{1}{2}$ " (ϕ 0.45 x 12mm) medical stainless-steel needle, and the duct was transferred into a perfusion chamber mounted on the stage of an IX71 inverted Olympus microscope (Olympus, Budapest, Hungary). Two concentric pipettes were used for the microperfusion of the ducts. The sealed end of the

duct was aspirated into the outer, holding pipette, then the inner, perfusion pipette, was gently inserted into the lumen while a negative pressure was applied to the holding pipette using a syringe. The duct was then perfused at a rate of 10-30 $\mu\text{l}/\text{min}$, the luminal perfusate left the duct at the open end. The high rate of the bath perfusion (5-6 ml/min), which was in the same direction as the flow of luminal perfusate, ensured that the outgoing luminal perfusate did not gain access to the basolateral surface of the duct cells. Replacement of the luminal perfusate took up to 2 minutes.

2.2.13. Measurement of intracellular calcium. Intracellular calcium concentration $[\text{Ca}^{2+}]_i$ was estimated using the Ca^{2+} -sensitive fluorescent dye FURA 2-AM. In the basolateral experiments sealed, cultured pancreatic ducts were attached to a glass coverslip (\varnothing 24 mm), using the cell adhesive Cell-Tak, forming the base of a perfusion chamber mounted on an Olympus microscope. The ducts were then bathed in the standard Hepes solution at 37 °C and loaded with the membrane permeable acetoxymethyl derivative of FURA 2 (5 $\mu\text{mol}/\text{L}$) for 60 min. After loading, the ducts were continuously perfused with solutions at a rate of 5-6 mL/min . In the microperfusion experiments, ducts were loaded first with 5 μmol FURA 2-AM in standard Hepes solution for 60 min and then microperfused as described above. $[\text{Ca}^{2+}]_i$ was measured using a Cell^R imaging system (Olympus, Budapest, Hungary) on 4-5 small areas (Region of interests – ROIs) of 5-10 cells in each intact duct. For excitation, 340 and 380 nm filters were used, and the changes in $[\text{Ca}^{2+}]_i$ were calculated from the fluorescence ratio (F_{340}/F_{380}) measured at 510 nm. One Ca^{2+}_i measurement was obtained per second.

2.2.14. Immunohistochemistry. The pancreatic tissues were fixed in 10% neutral buffered formalin for 24 hours. Paraffin embedded, 3-4 μm thick sections were used for immunohistochemistry. The slides were treated for 30 minutes with target retrieval solution (DAKO, Glostrup, Denmark) in a microwave oven, followed by incubation with the primary antibodies (Santa Cruz Biotechnology, Inc., Heidelberg, Germany) in 1:100 dilution at room temperature for 1 hour. PAR-2 antibody was a rabbit polyclonal antibody. Biotinylated secondary antibody (DAKO, LSAB kit) with diaminobenzidin (DAB) was used for visualization and counterstained with hematoxylin. Negative controls for nonspecific binding were incubated with secondary antibodies only, were processed and revealed no signal. Positive controls recommended by the manufacturer (Santa Cruz Biotechnology, Inc., Heidelberg, Germany) were used to confirm correct

immunohistochemical staining for PAR-2, that is normal brain. Reactions were scored positive where linear membrane staining was seen.

2.2.15. Ethics. All experiments were conducted in compliance with the *Guide for the Care and Use of Laboratory Animals* (U.S.A. NIH publication No 85-23, revised 1985). In addition, the experimental protocol was approved by the local Ethical Board of the University of Szeged, Hungary.

2.2.16. Statistics. The significance of the differences between CTRC mutation frequencies in affected individuals and controls were tested by two-tailed Fisher's Exact Test. Additional odds ratios were calculated using SAS/STAT software (v 9.1) and GraphPad Prism (v 4.03).

Results of the calcium measurements are expressed as means \pm S.E.M (n = 5 to 7 ducts / 20 to 35 ROIs). Statistical analyses were performed using ANOVA. P values \leq 0.05 were accepted as significant.

2.2.17. Accession codes. Entrez nucleotide: chymotrypsin C (CTRC): NT_004873 (chromosome 1 genomic contig); NM_007272 (human CTRC mRNA sequence); BI832476 (IMAGE clone used for plasmid construction). Protein Data Bank: chymotrypsinogen C crystal structure, 1PYT.

3. RESULTS

3.1. Purification of guinea pig trypsinogens.

Homogenate of guinea pig pancreas was applied to an ecotin-affinity column and the SDS-PAGE analysis of the given eluate revealed two closely migrating bands, a lighter upper band and a strong lower band, indicating that at least 2 different proteins were present in the ecotin eluate (Fig 1). To resolve these proteins, the ecotin eluate was loaded onto a Mono S cation-exchange column equilibrated with 20 mM Na-acetate (pH 5.0) and eluted with a NaCl gradient (0-0.5 M). A single major peak was eluted at approximately 0.15 M NaCl concentration (Fig 1A), which was identified as trypsinogen on the basis of its enzymatic activity after activation with enteropeptidase. In addition, a small, broader peak was eluted at approximately 0.22 M NaCl, which exhibited both trypsin and chymotrypsin activity upon activation with enteropeptidase or trypsin, respectively. Although not shown, the number of peaks eluted did not change when the NaCl gradient was extended to 1.0 M. Aliquots of fractions were analyzed by SDS-PAGE and Coomassie Brilliant Blue R-250 staining. The first, main peak showed only a single band, whereas the

second peak contained two bands, one of which co-migrated with the trypsinogen band recovered in the first peak (Fig 1B). Samples were shipped to Midwest Analytical Inc. for N-terminal sequencing. N-terminal sequencing of the first, major trypsinogen peak revealed a single, homogeneous sequence of Leu-Pro-Ile-Asp-Asp, suggesting that this peak contains a single trypsinogen isoform. This trypsinogen isoform was novel, as the N-

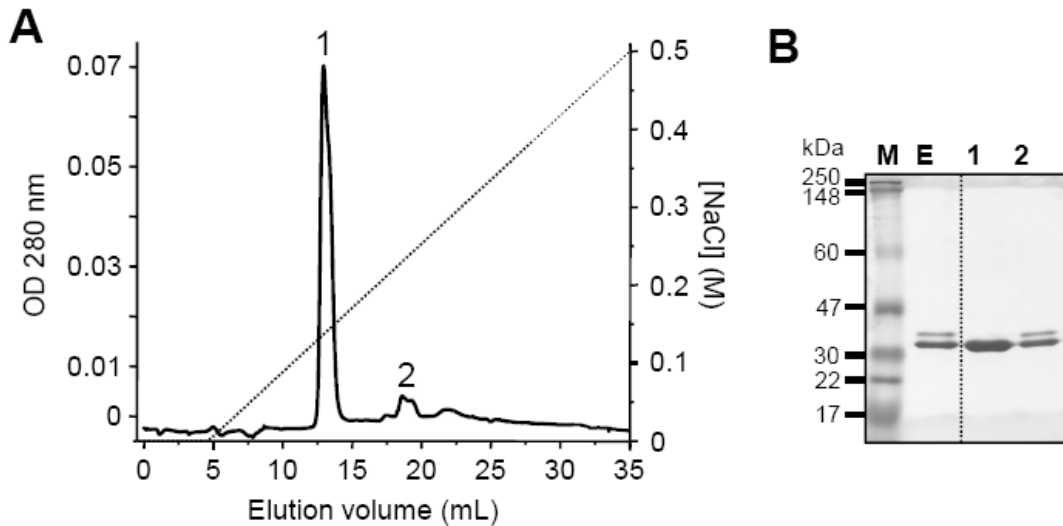


Figure 1. Purification of the guinea pig trypsinogen. (A) Mono S ion-exchange chromatogram of the guinea pig trypsinogens eluted from the ecotin affinity column. See text for details. The Mono S column was developed with a 0-0.5 M gradient of NaCl at a flow rate of 1 mL/min. (B) SDS-PAGE analysis of the ecotin-eluate (E, 50 μ L loaded; \sim 15 μ g protein) and Mono S peaks 1 and 2 (100 μ L from the 1 mL fraction loaded; \sim 15 μ g protein). Samples were precipitated with trichloroacetic acid (10 % final concentration); solubilized in reducing Laemmli sample buffer, heat-denatured, electrophoresed on 13 % minigels, and stained with Coomassie Brilliant Blue R-250. MultiMark multi-colored standards (Invitrogen) were used as molecular weight markers (M).

terminal sequence determined was distinct from the known trypsinogen sequences found in protein databases. The second peak contained a mixture of two different N-terminal sequences, a trypsinogen N terminus identical to the one found in the first, major peak and a chymotrypsinogen-like N terminal sequence of Cys-Gly-Val-Pro-Ala. Therefore, the enzyme activity assays and N terminal sequencing are in agreement demonstrating that the smaller Mono S peak contains a mixture of a trypsinogen and a chymotrypsinogen. The identical N-terminal sequences of the trypsinogens recovered in the first and second peaks suggested that the two peaks contained the same isoform and the small second trypsinogen peak represented an oligomeric or aggregate form of guinea pig trypsinogen. This conclusion was also supported by comparative MS/MS peptide sequencing of trypsinogens from the two peaks.

3.2. MS/MS peptide sequencing of purified guinea pig trypsinogen.

The previously mentioned two bands of the second peak of Mono S chromatogram (Fig 1.) were subjected to tandem MS (mass spectrometric) peptide sequencing by ProtTech, Inc, Eagleville, PA, USA (see also Methods 2.2.2). The following tryptic peptides were sequenced. LPIDDDDK (from Leu16 to Lys23); VSEGSEQFITASK (from Val80 to Lys92); HPSYSSSTLNNDIMLIK (from His96 to Lys112); and LASAANLNSK (from Leu113 to Lys122). Although this approach yielded about 20 % coverage of the protein sequence; the peptides sequenced were in perfect agreement with the amino-acid sequence predicted from the cloned cDNA. The trypsinogen band from the small, second Mono S peak was also subjected to MS/MS analysis and the exact same tryptic fragments were identified, confirming that this peak contained the same isoform of trypsinogen as the first main Mono S peak.

3.3. Complementary DNA cloning of guinea pig trypsinogens.

To determine the complete cDNA sequence of the guinea pig trypsinogen(s), we utilized a PCR-based cloning method after 5' and 3' RACE, as described in the *Methods*. The assembled cDNA sequences were essentially identical with the exception of 2 positions (Fig 2). Thus, at c.43 (in codon 15) a G/T variation was observed, whereas at c.276 (in codon 92) an A/G variation was found. The variant with c.43G and c.276A was arbitrarily designated as isoform 1 and the variant with c.43T and c.276G as isoform 2. The sequences of the 2 isoforms have been deposited with GenBank under accession numbers EF371801 and EF371802. The relative amounts of the two isoforms at the mRNA level appeared to be comparable, as judged from the isoform distribution of the sequenced 5' RACE clones. The G/T variation at codon 15 affects the encoded amino acid, which is predicted either as Ala (GCC) or Ser (TCC). In contrast, the G/A variation at position 92 has no affect at the protein level as both AAGG and AAAA codons encode for Lys. The deduced amino-acid sequences of the 2 isoforms differ only in amino-acid 15, which is either Ala or Ser. Position 15 is the last amino-acid of the secretory signal peptide, which is removed upon entry into the endoplasmic reticulum. The mature trypsinogens resulting from the two variants are thus identical, and the guinea pig pancreas secretes a single trypsinogen isoform.

The guinea pig pre-trypsinogens are composed of 246 amino acid residues, and the 231 amino-acid long mature trypsinogen has a predicted molecular weight of 24,378.5 Da.

The guinea pig trypsinogen is cationic in character, with a theoretical pI value of 8.0 (<http://ca.expasy.org/tools/protparam.html>). The N-terminal 15 amino acids form the signal peptide, which is followed by the 8 amino-acid long trypsinogen activation peptide including the highly conserved tetra-aspartate motif (Fig 2). Importantly, the predicted and experimentally determined N-terminal sequences of guinea pig trypsinogen are in perfect agreement. The molecule is stabilized by 6 disulfide bridges, characteristic of most vertebrate trypsinogens. Acidic determinants of the calcium-binding loop are also fully conserved (Glu75, Glu82 and Glu85). Similarly to human mesotrypsinogen, position 79 is Lys in the guinea pig trypsinogen, instead of the more typical Glu found in other mammalian trypsinogens. The functional role of this side-chain is unclear, but the Glu79→Lys mutation (E79K) in human cationic trypsinogen seems to be associated with chronic pancreatitis [57]. It is interesting to note that the otherwise highly conserved Arg122 is replaced with a Lys in the guinea pig trypsinogen. Arg122 is a trypsin sensitive site, which is believed to be important for autocatalytic degradation of bovine, rat and human trypsins [58, 59]. Mutation of Arg122 to His causes hereditary chronic pancreatitis in humans [28]. Relative to human trypsinogens, there is a low ratio of charged side-chains in the guinea pig trypsinogen (Arg, Lys, Asp and Glu residues; 11.3 % in guinea pig trypsinogen versus 18.1 % in both human trypsinogens), and a higher abundance of Ser residues (14.3 % in guinea pig trypsinogen versus 8.6 % and 10.3 % in human cationic and anionic trypsinogens, respectively). The guinea pig trypsinogen exhibits the strongest similarity to the bovine cationic trypsinogen (82 % identity), whereas the identity with human cationic and anionic trypsinogens are 76 % and 75 %, respectively.

1

TAC ATC GCC ACC ATG AAC GCA CTC CTG ATC CTA GCC CTT GTG GGA GCT GCT GTT ^T GCC
MÉT Asn Ala Leu Leu Ile Leu Ala Leu Val Gly Ala Ala Val Ala

16
TTG CCC ATT GAC GAT GAT GAC AAG ATC GTT GGG GGC TAT ACC TGC TCG GCA CAC TCC
Leu Pro Ile Asp Asp Asp Asp Lys Ile Val Gly Gly Tyr Thr Cys Ser Ala His Ser

35
GTT CCC TAC CAG GTG TCC CTG AAC AGT GGC TAC CAC TTC TGC GGC GGC TCC CTC ATC
Val Pro Tyr Gln Val Ser Leu Asn Ser Gly Tyr His Phe Cys Gly Gly Ser Leu Ile

54
AAT AAC CAA TGG GTG GTG TCT GCG GCT CAC TGC TAC AAG TCT CAG ATC CAA GTG AGA
Asn Asn Gln Trp Val Val Ser Ala Ala His Cys Tyr Lys Ser Gln Ile Gln Val Arg

73
CTG GGA GAG CAC AAC ATC AAA GTC TCG GAG GGG AGT GAA CAA TTT ATC ACT GCA AGC
Leu Gly Glu His Asn Ile Lys Val Ser Glu Gly Ser Glu Gln Phe Ile Thr Ala Ser
92G GP2 sense primer

AAA ATC ATC CGT CAT CCC AGC TAC AGC AGC AGC ACC CTG AAC AAT GAC ATC ATG CTG
Lys Ile Ile Arg His Pro Ser Tyr Ser Ser Ser Thr Leu Asn Asn Asp Ile Met Leu

111
ATC AAG CTC GCC TCA GCT GCA AAC CTC AAC TCC AAA GTG GCC GCT GTA TCT CTG CCC
Ile Lys Leu Ala Ser Ala Ala Asn Leu Asn Ser Lys Val Ala Ala Val Ser Leu Pro

130
TCC TCC TGT GTG TCT GCT GGC ACC ACA TGT CTC ATC TCT GGC TGG GGC AAC ACT CTG
Ser Ser Cys Val Ser Ala Gly Thr Thr Cys Leu Ile Ser Gly Trp Gly Asn Thr Leu

149
AGC TCT GGA GTC AAA AAC CCA GAC CTG CTG CAG TGC CTG AAT GCT CCT GTG CTT AGT
Ser Ser Gly Val Lys Asn Pro Asp Leu Leu Gln Cys Leu Asn Ala Pro Val Leu Ser

168
GP2 antisense primer
CAG TCT TCG TGT CAG TCC GCC TAT CCT GGA CAG ATC ACC AGC AAC ATG ATC TGC GTT
Gln Ser Ser Cys Gln Ser Ala Tyr Pro Gly Gln Ile Thr Ser Asn Met Ile Cys Val

187
GP1 sense and antisense primers
GGC TAC CTC GAG GGA GGC AAG GAT TCT TGC CAG GGT GAC TCT GGT GGC CCT GTG GTC
Gly Tyr Leu Glu Gly Gly Lys Asp Ser Cys Gln Gly Asp Ser Gly Gly Pro Val Val

206
TGC AAT GGG CAA CTC CAG GGC GTT GTC TCC TGG GGT TAT GGC TGT GCT CAG AAA AAC
Cys Asn Gly Gln Leu Gln Gly Val Val Ser Trp Gly Tyr Gly Cys Ala Gln Lys Asn

225
AAG CCT GGA GTG TAT ACC AAG GTG TGC AAC TAC GTG TCC TGG ATT CGA CAG ACC ATC
Lys Pro Gly Val Tyr Thr Lys Val Cys Asn Tyr Val Ser Trp Ile Arg Gln Thr Ile

244 246
GCT AGT AAC TGA GCC CCT AGT CCT GCT GCC ATC CCT ATG CCA ATA AAG TGA TCT GTG
Ala Ser Asn STOP

CTT G

Figure 2. Complementary DNA and deduced amino acid sequence of guinea pig pre-trypsinogens. Amino-acid numbering starts with the initiator methionine codon. Isoform 1 is shown, with the nucleotide differences present in isoform 2 indicated by purple superscripts. Note that Ala15 becomes Ser16 in isoform 2, whereas Lys92 remains unchanged. The sequences where the GP1 and GP2 primers anneal are underlined (grey). The highly conserved catalytic Ser200, typical of serine proteases, is highlighted in yellow. The activation peptide is shown in green.

3.4. Activation of guinea pig trypsinogen.

Activation characteristics and catalytic properties of guinea pig trypsinogen were compared to those of human anionic and cationic trypsinogens, which comprise 90-95 % of trypsinogens in humans. The physiological activator enteropeptidase readily activated guinea pig trypsinogen at pH 8.0, although at a rate that was slower than activation of

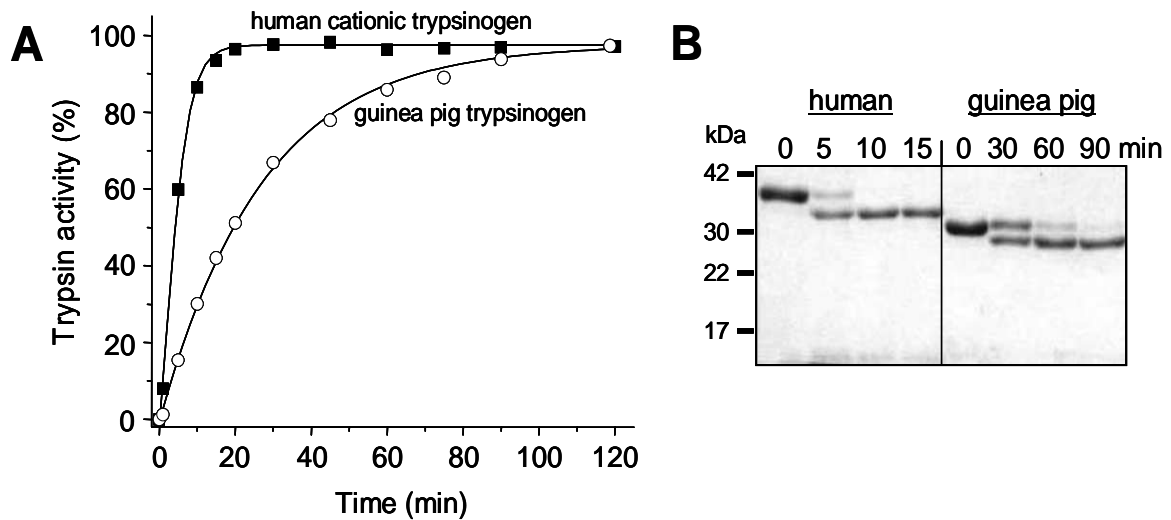


Figure 3. Activation of trypsinogen by enteropeptidase. (A) Approximately 2 μ M (final concentration) of guinea pig trypsinogen (open circles) and human cationic trypsinogen (solid squares) were incubated with 28 ng/mL enteropeptidase (final concentration) at 37 $^{\circ}$ C, in 0.1 M Tris-HCl (pH 8.0), 2 mg/mL bovine serum albumin and 1 mM CaCl_2 in a final volume of 100 μ L. Aliquots of 2 μ L were withdrawn from reaction mixtures at the indicated times, and trypsin activity was determined with the synthetic substrate *N*-CBZ-Gly-Pro-Arg-*p*-nitroanilide. Trypsin activity was expressed as a percentage of full activity. (B) Samples (100 μ L) were precipitated with 10 % trichloroacetic acid (final concentration) at the indicated times and analyzed by reducing SDS/PAGE (13%) and Coomassie Brilliant Blue R-250 staining.

human cationic trypsinogen (Fig 3). Similarly, activation of guinea pig trypsinogen by the pathological activator cathepsin B at pH 4.0 was slower, but still significant, relative to human cationic trypsinogen (Fig 4). Because we used human enteropeptidase and cathepsin B preparations in our experiments, the observed differences in activation rates between the human and guinea pig trypsinogens should be interpreted cautiously. The important conclusion of the experiments in Figs. 3 and 4 is that both enteropeptidase and cathepsin B can activate guinea pig trypsinogen under certain conditions.

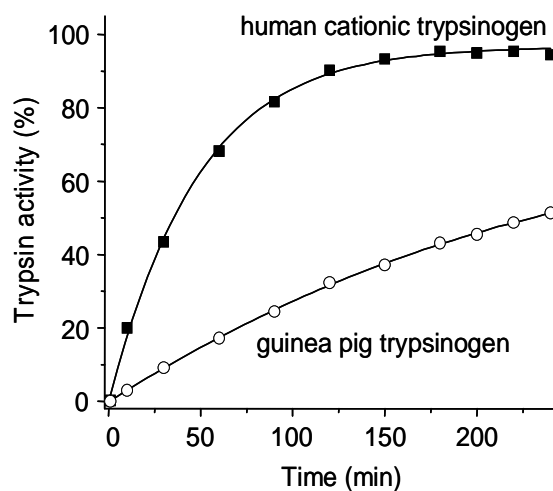


Figure 4. Activation of trypsinogen by cathepsin B. Guinea pig trypsinogen (open circles) and human cationic trypsinogen (solid squares) were activated at 2 μ M concentration with human cathepsin B (90 μ g/mL) at 37 $^{\circ}$ C in 0.1 M sodium acetate buffer (pH 4.0) in the presence of 1 mM dithiothreitol, 2 mg/mL bovine serum albumin, 1 mM K-EDTA and 0.3 mM benzamidine. Aliquots (2 μ L) were withdrawn at indicated times and trypsin activity was measured on the synthetic substrate.

In contrast, a completely different picture emerged when autoactivation of guinea pig trypsinogens and human trypsinogens were compared. Human anionic and cationic trypsinogens autoactivated rapidly, whereas guinea pig trypsinogen exhibited essentially no autoactivation (Fig 5).

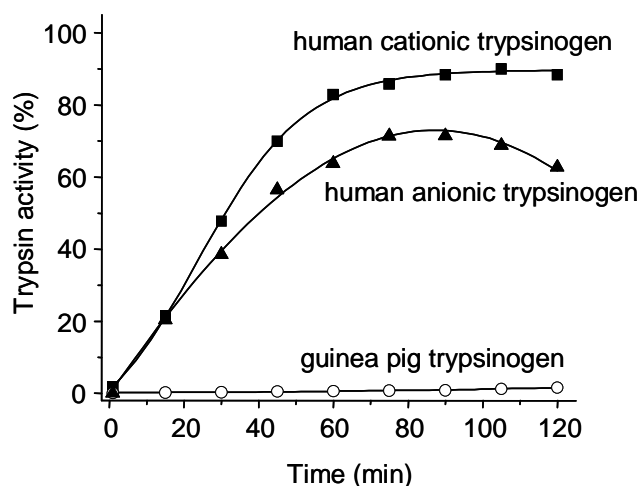


Figure 5. Trypsin-mediated trypsinogen activation (autoactivation). Guinea pig trypsinogen (open circles), human cationic trypsinogen (solid squares) and human anionic trypsinogen (solid triangles) were activated with their respective trypsins. The reactions were carried out at 37 °C, using 2 μ M trypsinogen, 1 mM CaCl_2 , 0.1 M Tris-HCl (pH 8.0), and 200 nM trypsin initial concentrations. Although not shown, increasing the CaCl_2 concentration to 10 mM had no measurable stimulatory effect on the autoactivation of guinea pig trypsinogen in this time range.

3.5. Catalytic activity and autolysis of guinea pig trypsin.

Catalytic parameters of guinea pig trypsin were determined on the peptide substrate N-CBZ-Gly-Pro-Arg-p-nitroanilide. The k_{cat} and K_M values were similar to those of human trypsins, indicating that lack of autoactivation (see above) was not due to a catalytic defect in guinea pig trypsin (Table 2.).

	k_{cat} (s^{-1})	K_M (μM)	k_{cat}/K_M ($\text{M}^{-1}\cdot\text{s}^{-1}$)
guinea pig	115.6	14.6	7.9×10^6
human cationic	85.3	17.6	4.8×10^6

Table 2. Kinetic parameters of guinea pig trypsin and human cationic trypsin on the synthetic substrate N-CBZ-Gly-Pro-Arg-p-nitroanilide.

Autocatalytic degradation (autolysis) of guinea pig trypsin was also measured. Figure 6 demonstrates that at pH 8.0, in the absence of Ca^{2+} , the guinea pig trypsin underwent relatively slow autolysis at an intermediate rate between those of the two human trypsins. As observed previously, human cationic trypsin was resistant to autolysis, whereas anionic trypsin rapidly autodegraded [60, 61].

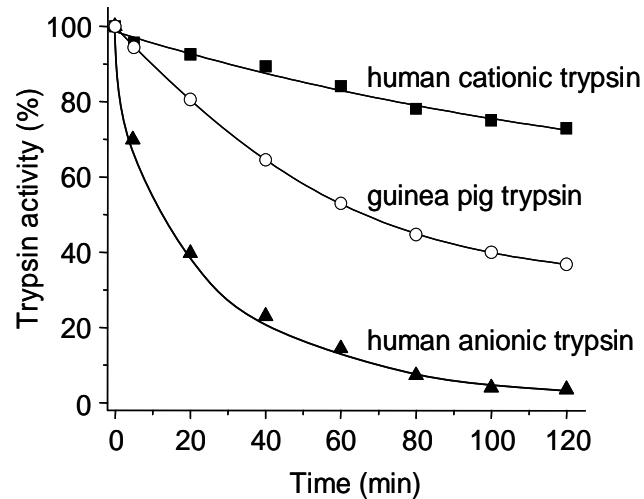


Figure 6. Autocatalytic degradation (autolysis) of trypsin. Guinea pig trypsinogen (open circles), human cationic trypsinogen (solid squares), and human anionic trypsinogen (solid triangles) were activated at $2 \mu\text{M}$ concentration with enteropeptidase for 60 min at 37°C in the presence of 1 mM CaCl_2 . Autocatalytic inactivation of trypsins was then followed at 37°C after addition of K-EDTA (pH 8.0) to a final concentration of 2 mM . Residual activities were expressed as percentage of the full trypsin activity measured after enteropeptidase activation.

3.6. DNA sequencing of the human chymotrypsin C gene.

We carried out direct DNA sequencing of all eight exons of the 8.2-kb chymotrypsin (CTRC) gene in 621 individuals with idiopathic or hereditary chronic pancreatitis and in 614 control subjects of German origin (see Method 2.2.5.). We found several *CTRC* variants, the large majority of which affected exons 2, 3 and 7. Therefore, we extended our analyses by sequencing an additional 280 affected individuals for these three exons and an additional 2,075 controls for exons 2 and 3 and 2,190 controls for exon 7. Altogether, we identified 11 missense and 2 deletion variants in *CTRC* (Table 3). The two most frequent variants, c.760C4T (p.R254W) and c.738_761del24 (p.K247_R254del), both located in exon 7, were found in affected individuals with a frequency of 2.1% and 1.2%, respectively. Taken together, the two alterations were significantly overrepresented in the pancreatitis group (30 of 901; 3.3%) compared to controls (21 of 2,804; 0.7%) (OR = 4.6; CI = 2.6–8.0; $P = 1.3 \times 10^{-7}$). Variant c.738_761del24, which causes an in-frame deletion of eight amino acids from Lys247 through Arg254 (p.K247_R254del), showed the strongest disease association (OR = 11.5; CI = 3.2–41.5; $P = 0.00003$). Subgroup analysis

for these two heterozygous variants showed similar frequency in the hereditary (6 of 143; 4.2%; 6 _ p.R254W) and idiopathic (24 of 758; 3.2%; 13 _ p.R254W; 11 _ p.K247_R254del) groups (Table 3). One individual with idiopathic disease was compound heterozygous for p.V235I (inherited from the mother) and p.R254W (inherited from the father).

Exon	Nucleotide change	Amino acid change	Affected individuals (ICP)	Affected individuals (HP)	Affected individuals (all)	Controls	P value	OR	95% CI
2	c.103G>C	p.D35H	0/758 (0%)	0/143 (0%)	0/901 (0%)	1/2689 (0.04%)	1.0	-	-
2	c.103G>A	p.D35N	0/758 (0%)	0/143 (0%)	0/901 (0%)	1/2689 (0.04%)	1.0	-	-
2	c.110G>A	p.R37Q	5/758 (0.7%)	1/143 (0.7%)	6/901 (0.7%)	10/2689 (0.4%)	0.25	-	-
3	c.143A>G	p.Q48R	0/758 (0%)	2/143 (1.4%)	2/901 (0.2%)	1/2689 (0.04%)	0.16	-	-
4	c.308delG	p.G103VfsX31	0/499 (0%)	1/122 (0.8%)	1/621 (0.2%)	0/614 (0%)	1.0	-	-
6	c.514A>G	p.K172E	0/499 (0%)	0/122 (0%)	0/621 (0%)	1/614 (0.2%)	0.5	-	-
7	c.649G>A	p.G217S	2/758 (0.3%)	0/143 (0%)	2/901 (0.2%)	1/2804 (0.04%)	0.15	-	-
7	c.652G>A	p.G218S	0/758 (0%)	0/143 (0%)	0/901 (0%)	1/2804 (0.04%)	1.0	-	-
7	c.659T>G	p.L220R	0/758 (0%)	0/143 (0%)	0/901 (0%)	1/2804 (0.04%)	1.0	-	-
7	c.674A>C	p.E225A	0/758 (0%)	0/143 (0%)	0/901 (0%)	1/2804 (0.04%)	1.0	-	-
7	c.703G>A	p.V235I	1/758 (0.1%)	0/143 (0%)	1/901 (0.1%)	1/2804 (0.04%)	0.43	-	-
7	c.760C>T	p.R254W	13/758 (1.7%)	6/143 (4.2%)	19/901 (2.1%)	18/2804 (0.6%)	0.0004*	3.3	1.7-6.4
7	c.738_761del ₂₄	p.K247_R254del	11/758 (1.5%)	0/143 (0%)	11/901 (1.2%)	3/2804 (0.1%)	0.00003*	11.5	3.2-41.5

P values were determined by Fisher's Exact Test. * all affected individuals against controls

ICP, idiopathic chronic pancreatitis; HP, hereditary chronic pancreatitis

Table 3. CTRC variants detected in German subjects with idiopathic or hereditary chronic pancreatitis and healthy controls.

To confirm our findings in an independent cohort affected with another inflammatory pancreatic disease, we sequenced all eight exons of *CTRC* in 96 German individuals affected with alcohol-related chronic pancreatitis. Subsequently, we sequenced exons 2, 3 and 7 in an additional 252 subjects (348 subjects in total) with alcoholic chronic pancreatitis. For controls, we analyzed exons 2, 3 and 7 in 432 German individuals with alcoholic liver disease but without chronic pancreatitis. Again, we found a significant enrichment of the two exon 7 variants, p.R254W and p.K247_R254del, in subjects with alcoholic pancreatitis (10 of 348; 2.9%) versus subjects with alcohol-related liver disease (3 of 432; 0.7%) (OR = 4.2; CI = 1.2–5.5; P = 0.02; Table 4).

Exon	Nucleotide change	Amino acid change	Affected individuals	Controls	P value	OR	95% CI
2	c.110G>A	p.R37Q	0/348 (0%)	3/432 (0.7%)	0.26	-	-
7	c.649G>C	p.G217R	1/348 (0.3%)	0/432 (0%)	0.45	-	-
7	c.703G>A	p.V235I	1/348 (0.3%)	1/432 (0.2%)	1.0	-	-
7	c.746C>T	p.P249L	1/348 (0.3%)	0/432 (0%)	0.45	-	-
7	c.760C>T	p.R254W	8/348 (2.3%)	2/432 (0.5%)	0.03	5.1	1.1-24.0
7	c.738_761del24	p.K247_R254del	2/348 (0.6%)	1/432 (0.2%)	0.58		

P values were determined by Fisher's Exact Test.

Table 4. *CTRC* variants detected in German subjects with alcohol-related chronic pancreatitis and controls with alcoholic liver disease without pancreatitis.

Finally, to investigate the significance of *CTRC* variants in chronic pancreatitis in subjects of non-European descent, we analyzed 71 individuals affected with tropical pancreatitis and 84 controls of Indian origin. Notably, the frequency of *CTRC* alterations in subjects with pancreatitis was even higher in this cohort (Table 5).

Exon	Nucleotide change	Amino acid change	Affected individuals	Controls	P value	OR	95% CI
3	c.190_193delATTG	p.I64LfsX69	2/71 (2.8%)	0/84 (0%)	0.21	-	-
3	c.217G>A	p.A73T	4/71 (5.6%)	0/84 (0%)	0.04	11.3	0.6-213
7	c.703G>A	p.V235I	1/71 (1.4%)	0/84 (0%)	0.46	-	-
7	c.760C>T	p.R254W	2/71 (2.8%)	1/84 (1.2%)	0.60	-	-
7	c.778G>A	p.D260N	1/71 (1.4%)	0/84 (0%)	0.46	-	-
All			10/71 (14.1%)	1/84 (1.2%)	0.0028	13.6	1.7-109.

P values were determined by Fisher's Exact Test.

Table 5. *CTRC* variants detected in subjects with tropical pancreatitis and healthy controls of Indian origin.

Overall, 14.1% of affected individuals but only 1.2% of controls carried a *CTRC* variant (OR = 13.6; CI = 1.7–109.2; P = 0.0028). Two relatively frequent variants found in Indians were absent in Germans: the c.217G4A (p.A73T) missense alteration and the c.190_193delATTG (p.I64LfsX69) frameshift deletion. On the other hand, the p.K247_R254del variant that was relatively frequent in affected individuals from Germany was not found in the Indian population, and the enrichment of the p.R254W variant in subjects with tropical pancreatitis did not reach statistical significance. However, because

of the significantly smaller size of the Indian cohort relative to the German cohort, caution is warranted in the interpretation of these differences. Nonetheless, the data clearly indicate that *CTRC* variants increase the risk for tropical pancreatitis as well.

3.7. Examination of the effects of pancreatitis associated CTRC variants on the secretion of chymotrypsinogen C.

To investigate the functional consequences of the *CTRC* missense alterations and the p.K247_R254del in-frame deletion, we expressed wild-type and mutant *CTRC* in HEK 293T cells via transient transfection. Strikingly, secretion of p.K247_R254del and p.A73T was severely diminished relative to the wild-type, as evidenced by the loss of *CTRC* activity in enzyme assays and the faint protein bands on gels (Fig 7A and 7B). When these two mutants were partially purified to test their activity, p.K247_R254del proved catalytically inactive, whereas p.A73T exhibited measurable protease activity (data not shown). In contrast to the almost complete loss of function observed with p.K247_R254del and p.A73T, *CTRC* activity secreted by cells expressing the p.R254W mutant was reduced to about 40% of wild-type (Fig 7A). SDS-PAGE of conditioned media revealed that secreted levels of p.R254W were about 50% less than wild-type *CTRC*, suggesting that the functional defect in this mutant is decreased secretion rather than impaired catalytic activity (Fig 7B). This conclusion was strengthened by enzyme kinetic analysis of purified wild-type and p.R254W mutant *CTRC*. Kinetic parameters compared on two different chromogenic peptide substrates were essentially identical (Table 6), indicating that reduced function of p.R254W is solely due to decreased secretion.

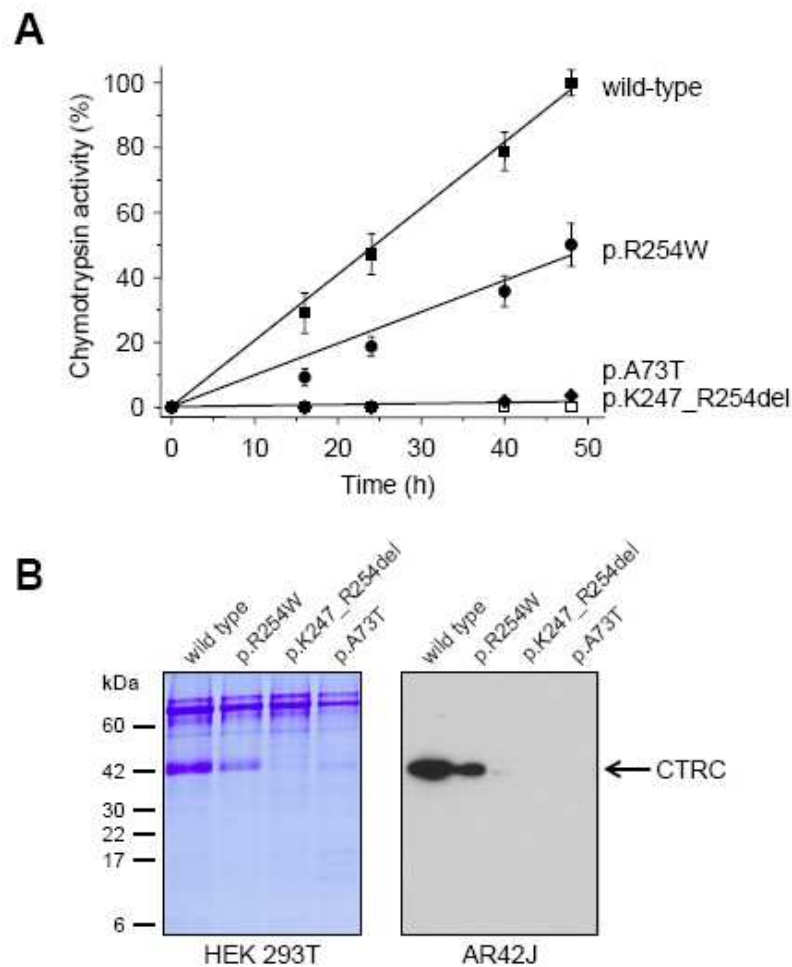


Figure 7. Effects of pancreatitis associated CTRC variants on the secretion of chymotrypsinogen C. (A) HEK 293T cells were transfected with the indicated constructs, and aliquots of conditioned media were withdrawn at the given times. CTRC activity was determined after activation with trypsin, as described in the *Methods*, and expressed as percentage of the maximal activity, which corresponded to 14.7 μM p-nitroaniline released per minute. (B) Aliquots (0.15 mL) of conditioned media of transfected HEK 293T cell were precipitated with 10% trichloroacetic acid (final concentration) and analyzed by SDS-PAGE and Coomassie Brilliant Blue R-250 staining (left panel). Alternatively, AR42J cells were transfected with Glu-Glu tagged versions of wild-type and mutant CTRC constructs and conditioned media were analyzed by Western blotting using an antibody against the Glu-Glu tag.

Suc-Ala-Ala-Pro-Phe-p-nitroanilide

	wild type	R254W
K_M	$10.3 \pm 0.4 \mu\text{M}$	$11.0 \pm 1.1 \mu\text{M}$
k_{cat}	$4.7 \pm 0.1 \text{ s}^{-1}$	$4.1 \pm 0.1 \text{ s}^{-1}$
k_{cat}/K_M	$4.6 \cdot 10^5 \text{ M}^{-1} \text{ s}^{-1}$	$3.7 \cdot 10^5 \text{ M}^{-1} \text{ s}^{-1}$

Glt-Ala-Ala-Pro-Leu-p-nitroanilide

	wild type	R254W
K_M	$2.3 \pm 0.2 \mu\text{M}$	$3.9 \pm 0.5 \mu\text{M}$
k_{cat}	$2.3 \pm 0.1 \text{ s}^{-1}$	$2.2 \pm 0.1 \text{ s}^{-1}$
k_{cat}/K_M	$1.0 \cdot 10^6 \text{ M}^{-1} \text{ s}^{-1}$	$5.6 \cdot 10^5 \text{ M}^{-1} \text{ s}^{-1}$

Table 6. Kinetic parameters of wild-type CTRC and mutant p.R254W on chromogenic peptide substrates in 0.1 M Tris-HCl (pH 8.0), 1 mM CaCl_2 , at room temperature.

To demonstrate that the clinically significant *CTRC* mutants are also poorly secreted in cells that more closely resemble human pancreatic acinar cells, we performed additional transfection experiments with the AR42J rat acinar cell line [62]. Wild-type *CTRC* and mutants p.A73T, p.K247_R254del and p.R254W were tagged with a Glu-Glu affinity tag to allow specific detection in the background of the native chymotrypsinogens secreted by AR42J cells. Stimulation of transfected cells with the cholecystokinin analog cerulein resulted in secretion of immunoreactive wild-type and somewhat less p.R254W mutant, whereas p.A73T and p.K247_R254del were not secreted to detectable levels (Fig 7B).

In addition to the frequent *CTRC* alterations mentioned above, we also analyzed the variants p.R37Q, p.Q48R, p.G217S, and p.V235I by transient transfections in HEK 293T cells (Fig 8). Variant p.R37Q exhibited essentially normal activity and secretion (~82-88 % of wild-type). In contrast, no *CTRC* activity was measurable from conditioned media of cells transfected with mutant p.Q48R and SDS-PAGE revealed a significant secretion defect (~30 % of wild type). We also found that mutant p.Q48R underwent degradation during trypsin-mediated activation, presumably because the mutation introduced a new trypsin sensitive site (not shown). Mutant p.G217S showed significant catalytic impairment (specific activity only ~7 % of wild type) and a modest decrease in secretion (~70 % of wild type). Finally, *CTRC* activity secreted by cells transfected with variant p.V235I was moderately reduced (~65 % of wild type); which seemed to be due to a combination of slightly lower specific activity and slightly reduced secretion of *CTRC* protein. Figure 9 summarizes the secretion of all the examined chymotrypsinogen C variants in percentage relative to wild type (Fig 9).

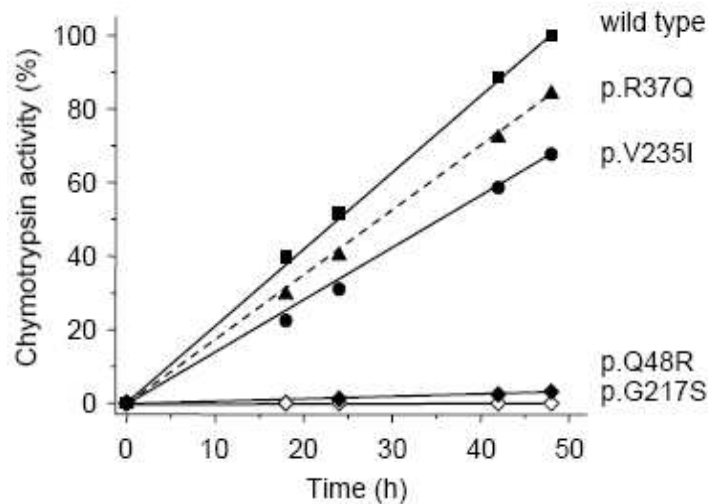


Figure 8. Effect of different CTRC variants on chymotrypsinogen C secretion. HEK 293T cells were transfected with the indicated constructs, and CTRC activity in the conditioned media was determined as described in the legend to Fig. 7 .

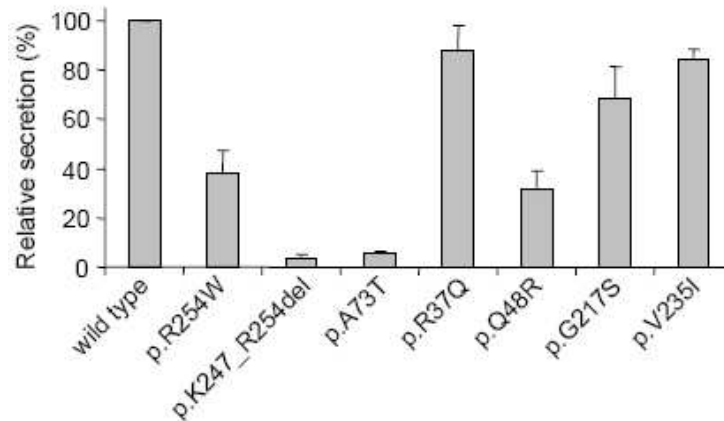


Figure 9. Summary of secretion of chymotrypsinogen C variants relative to wild type. The amount of secreted CTRC protein was determined by densitometry of dried gels stained with Coomassie Brilliant Blue R-250. Gels were scanned at 300 dpi resolution and CTRC bands were quantitated using the Volume Analysis tool of the Bio-Rad Quantity One software (ver. 4.4.0). The average of at least 3 experiments is shown; the standard deviation was within 15 %.

3.8. Molecular modeling of the CTRC mutations.

Molecular modeling indicates that p.K247_R254del eliminates the last of the 6 β -strands of the C-terminal antiparallel β -barrel domain (Fig 10). A change of this magnitude in a structurally conserved part is expected to cause a folding defect, which might lead to the observed loss of catalytic function and the diminished secretion. Interestingly, p.R254W is also found within this deleted peptide segment. Variant p.A73T is located next to the catalytic His74 (His57 in the conventional chymotrypsin numbering), and thus might interfere with enzyme function. However, we found that the loss of function in p.A73T was caused by a marked secretion defect rather than catalytic impairment. Inspection of the atomic model reveals that Ala73 is in the vicinity of two hydrophobic side-chains, Trp113

and Val109, suggesting that replacement of Ala73 by the more bulky and polar threonine results in unfavorable interactions with the surrounding hydrophobic residues and thereby in altered folding with consequent intracellular retention and degradation.

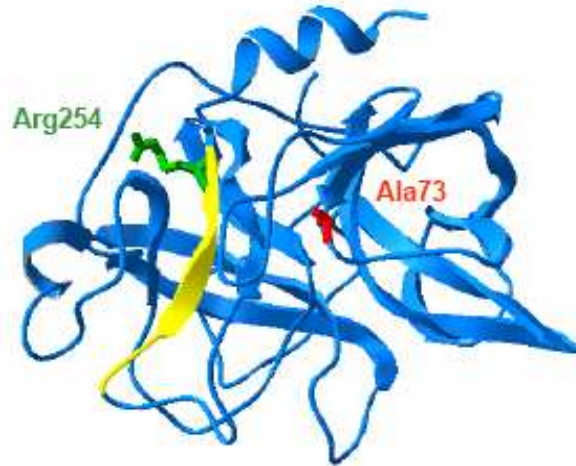


Figure 10. Ribbon diagram of chymotrypsinogen C. The bovine chymotrypsinogen C molecule is shown, which was crystallized as part of a ternary complex with proproteinase E and procarboxypeptidase A (Protein Data Bank file 1PYT). The position of Ala73 (mutated in p.A73T) is shown in red and Arg254 (mutated in p.R254W) is indicated in green. The yellow peptide segment is deleted in mutant p.K247_R254del. The image was rendered using DeepView/Swiss-PdbViewer v. 3.7 (www.expasy.org/spdbv/).

3.9. Effect of trypsin and bile acids on the calcium signalling of pancreatic duct epithelial cells.

It has been previously shown that activation of PAR-2 regulates the calcium signalling of pancreatic duct cells [43], so we performed experiments to reveal whether trypsin stimulates guinea pig pancreatic duct epithelial cells. Basolateral administration of trypsin dose-dependently triggered intracellular calcium release in the pancreatic duct cells, which showed a sharp initial peak followed by a rapid decrease (Fig 11A-E).

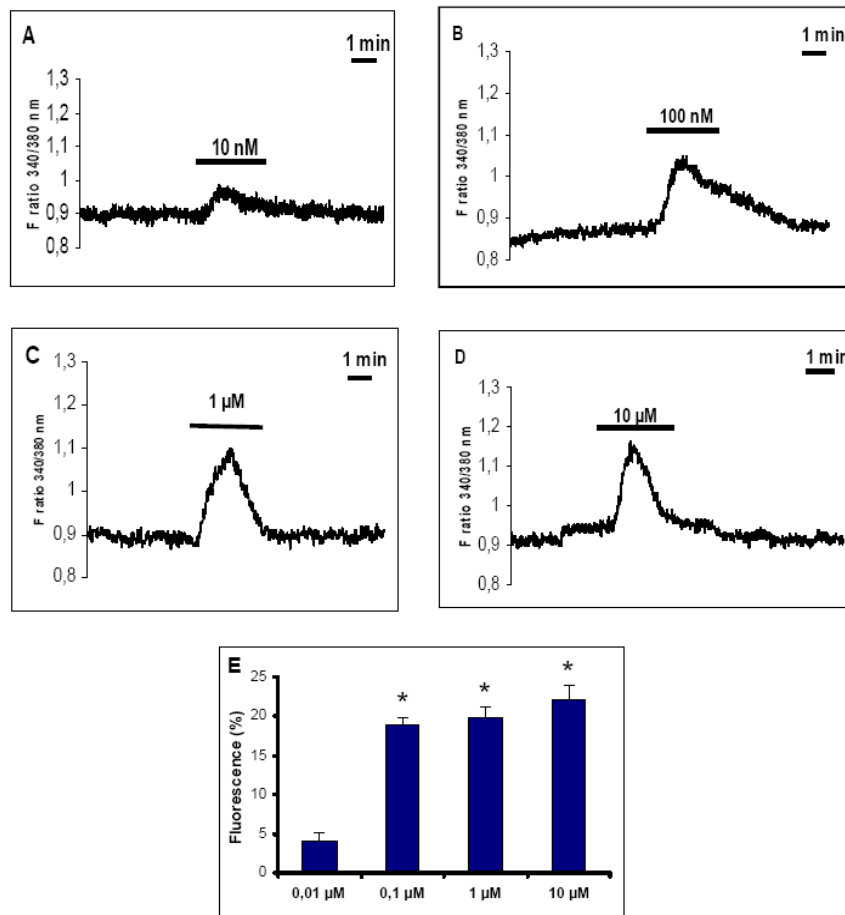


Figure 11. Trypsin increases intracellular calcium concentration in guinea pig pancreatic duct cells. (A-D) Representative traces show the effects of trypsin, which triggers dose-dependent calcium signals (10 nM-10 μM). **(E)** The bar chart shows the summary of results. Means ± SEM are from 4-6 individual ducts. *: p<0.001 vs. 0.01 μM.

The effect of trypsin on increase in $[Ca^{2+}]_i$ was totally blocked by soybean trypsin inhibitor (1mg/ml) (Fig 12A) and the Ca^{2+} -chelator BAPTA-AM (20 μ M) (Fig 12B). The removal of calcium from the extracellular solution did not reduce the rise in $[Ca^{2+}]_i$ evoked by trypsin (Fig 12C). PAR-2 activating peptide (0.3 mM) could mimic the effect of the stimulatory effect of basolateral administration of trypsin (Fig 12D). Luminal administration of trypsin performed by the microperfusion technique (see Methods 2.2.12.) also caused calcium response in the cells, although, the registered calcium signal was lower and had a well-sustained plateau after the initial peak compared to the signals triggered by basolateral trypsin (Fig 12E).

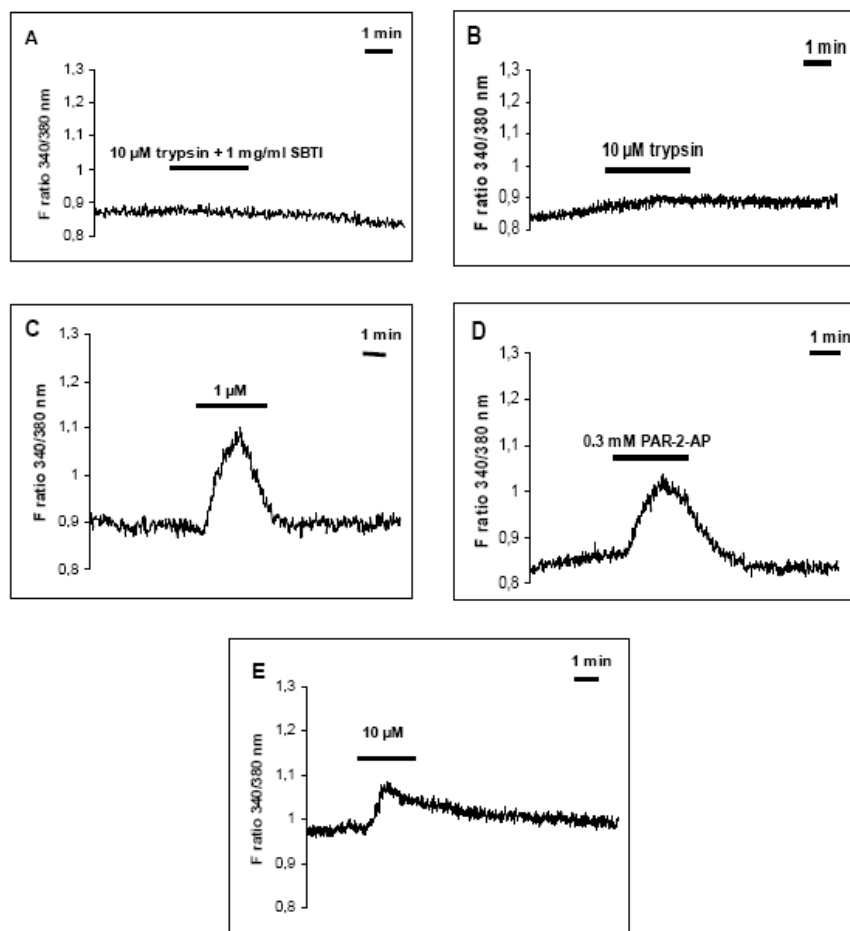


Figure 12. The effects of trypsin on $[Ca^{2+}]_i$ under different conditions. (A) Effect of basolateral trypsin after pretreatment of the 10 μ M trypsin solution with 1 mg/ml (0.05 μ M) soybean trypsin inhibitor (SBTI) for 30 min at room temperature. (B) Pretreatment of the duct cells with the calcium chelator BAPTA-AM (20 μ M) for 30 min blocked the calcium response. (C) Deprivation of Ca^{2+} from the external solution did not modify the effects of trypsin on $[Ca^{2+}]_i$. (D) PAR-2 activating peptide mimicked the effect of trypsin. (E) Luminal administration of trypsin. The traces are representative of experiments performed on 4-7 individual ducts.

PAR-2 expression has been detected in dog [43], bovine [44] and human pancreatic duct cells [45]. We performed immunostaining of the guinea pig pancreas to identify PAR-2 expressing cells. Surprisingly, pancreatic duct cells showed differential expression of PAR-2, as the receptor was expressed on the luminal membrane of intralobular ducts (Fig 13A) but not in interlobular ducts, where PAR-2 was found in periductal nerves (Fig 13B). The receptor has also been detected in endothelial cells (Fig 13C) and in Langerhans islets (Fig 13D).

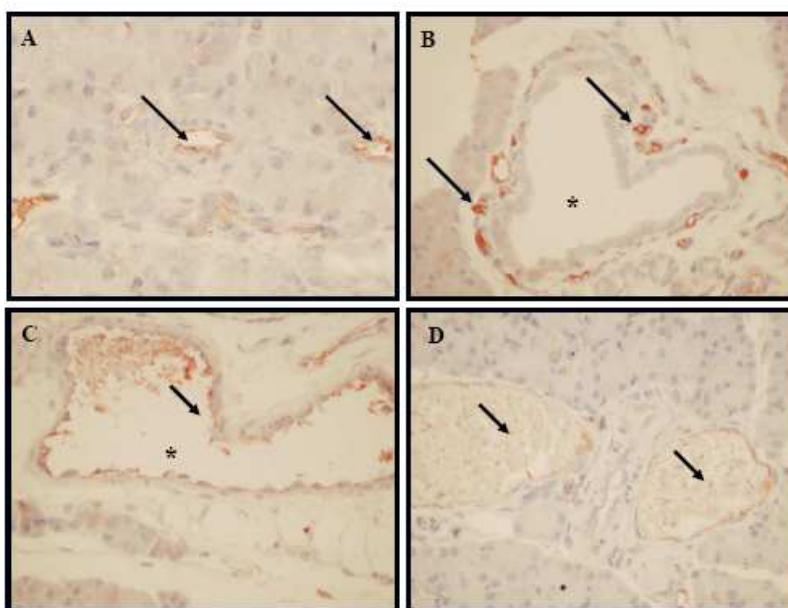


Figure 13. Localization of PAR-2 by immunohistochemical staining of the sections of the intact guinea pig pancreas using anti-PAR-2 antibody. (A) Expression of PAR-2 on the luminal membrane of intralobular ducts of the guinea pig pancreas (600x). The arrows indicate intensely stained cells. (B) Expression of PAR-2 in periductal nerves around interlobular ducts (600x). Asterisks denote the lumen of the pancreatic duct. Localization of PAR-2 in (C) endothelial cells (600x) and (D) Langerhans islets (600x). The asterisk on figure 13C denote the lumen of a pancreatic blood vessel.

We also examined whether bile acids can activate the calcium signalling mechanisms of pancreatic duct epithelial cells. Bile acids have been shown to evoke Ca^{2+} signalling in pancreatic acinar cells [35], therefore, we thought to test whether bile acids have any effect on $[Ca^{2+}]_i$ in guinea pig pancreatic ducts.

Figure 14A and B show that basolateral administration of chenodeoxycholate and glycochenodeoxycholate caused a dose-dependent increase in $[Ca^{2+}]_i$ (Figs 14A and B). The unconjugated chenodeoxycholate was the most effective, causing what appeared to be repetitive $[Ca^{2+}]_i$ transients at a dose of 0.1 mM and a large initial peak in $[Ca^{2+}]_i$ followed by a sustained plateau at 1 mM (Fig 14A). In contrast, 0.1 mM of the conjugated glycochenodeoxycholate had little or no effect on $[Ca^{2+}]_i$ while 1 mM

glycochenodeoxycholate caused a small initial peak followed by a sustained plateau which was similar in magnitude to the plateau obtained with 1 mM chenodeoxycholate (Fig 14B).

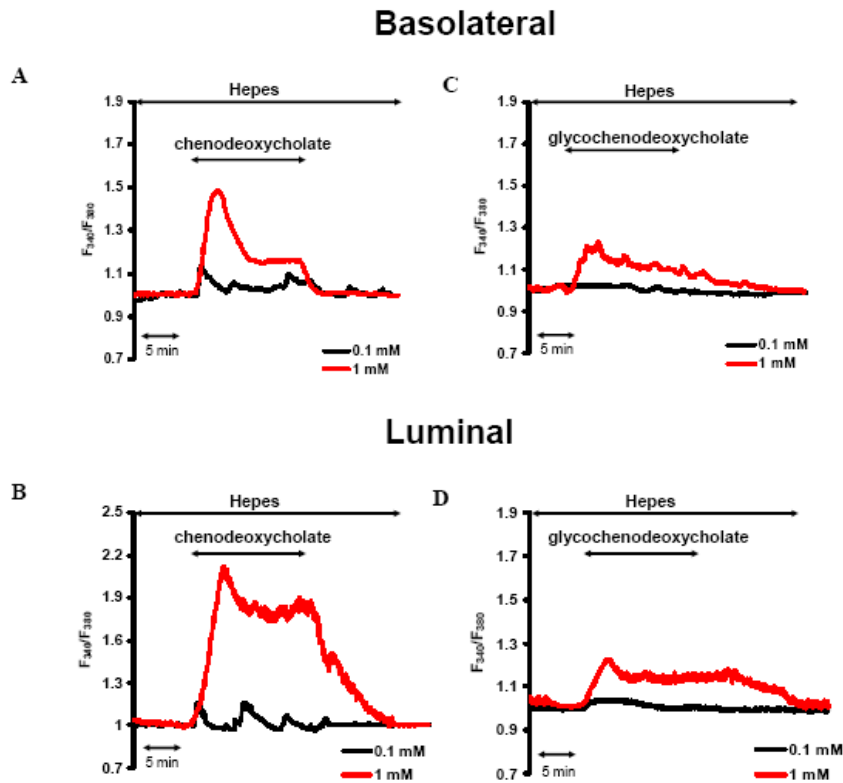


Figure 14. Bile acids stimulate calcium signalling in guinea pig pancreatic ducts. The effect of basolateral (A,C) and luminal (B,D) 0.1-1 mM chenodeoxycholate (A,B) or glycochenodeoxycholate (C,D) on intracellular calcium concentration $[Ca^{2+}]_i$ in standard HEPES solution. Chenodeoxycholate and glycochenodeoxycholate dose-dependently increased the $[Ca^{2+}]_i$ in each experiment. (B) 1 mM chenodeoxycholate caused the highest elevation in $[Ca^{2+}]_i$ from the luminal membrane, while the low dose of glycochenodeoxycholate had only a slight effect on $[Ca^{2+}]_i$ from the luminal membrane (D).

Luminal application of 0.1 mM chenodeoxycholate caused slow $[Ca^{2+}]_i$ transients which appeared to decline during continued exposure to the bile acid. However, 1.0 mM luminal chenodeoxycholate caused a very large sustained increase in $[Ca^{2+}]_i$ (Fig 14B). In contrast, 0.1 mM of the conjugated glycochenodeoxycholate had no effect on $[Ca^{2+}]_i$ when applied from the lumen whereas 1 mM caused a rise in $[Ca^{2+}]_i$ comparable to that observed when the same dose was applied from the basolateral membrane (compare figs. 14C and 14D).

Figure 15 shows fluorescent ratio images of perfused pancreatic ducts exposed to chenodeoxycholate, which confirm the results described above. Basolateral application of 0.1 mM chenodeoxycholate caused localized increases in $[Ca^{2+}]_i$ within the duct, whereas all cells appeared to be affected by 1 mM chenodeoxycholate. Following luminal application, localized increases in $[Ca^{2+}]_i$ were also observed with 0.1 mM

chenodeoxycholate, but these were more extensive compared to when the same dose was administered basolaterally. Luminal 1 mM chenodeoxycholate caused a very large generalized increase in $[Ca^{2+}]_i$.

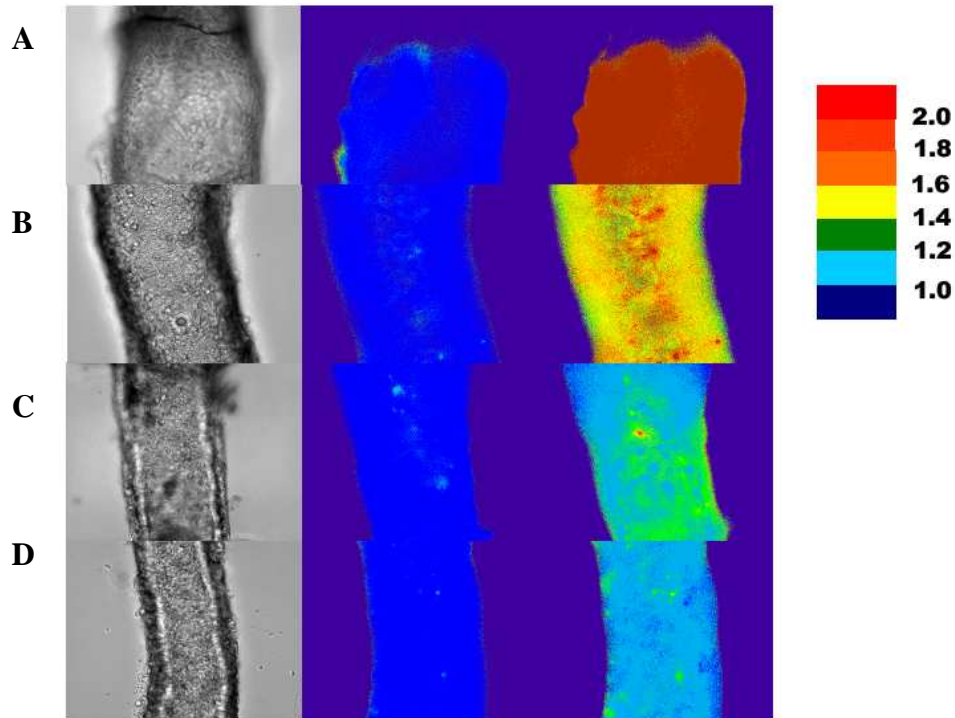


Figure 15. Light and fluorescent ratio images of pancreatic ducts perfused with either 1 (panel A and B) or 0.1 mM (panel C and D) chenodeoxycholate from either the luminal (panel A and C) or basolateral side (panel B and D). An increase in $[Ca^{2+}]_i$ is denoted by a change from a “cold” color (blue) to a “warmer” color (yellow to red); see scale on the right. Fluorescent pictures (in middle and on the right side) were taken before and 1 min after exposure of the ducts to chenodeoxycholate.

Neither atropine (100 μ M) nor removal of extracellular Ca^{2+} had any effect on the $[Ca^{2+}]_i$ rise evoked by basolateral administration of chenodeoxycholate (Fig 16A). However, the IP_3 receptor antagonist caffeine (20 mM), the Ca^{2+} -chelator BAPTA-AM (40 μ M), the IP_3 receptor inhibitor xestospongine C (50 μ M) and the phospholipase C inhibitor U73122 (10 μ M) all completely blocked the rise in $[Ca^{2+}]_i$ evoked by 0.1 mM chenodeoxycholate (Fig 16A). The inhibitors also reduced, albeit less so, the rise in $[Ca^{2+}]_i$ evoked by 1 mM basolateral chenodeoxycholate (Fig 16B). Similar results were obtained when chenodeoxycholate was applied from the luminal membrane.

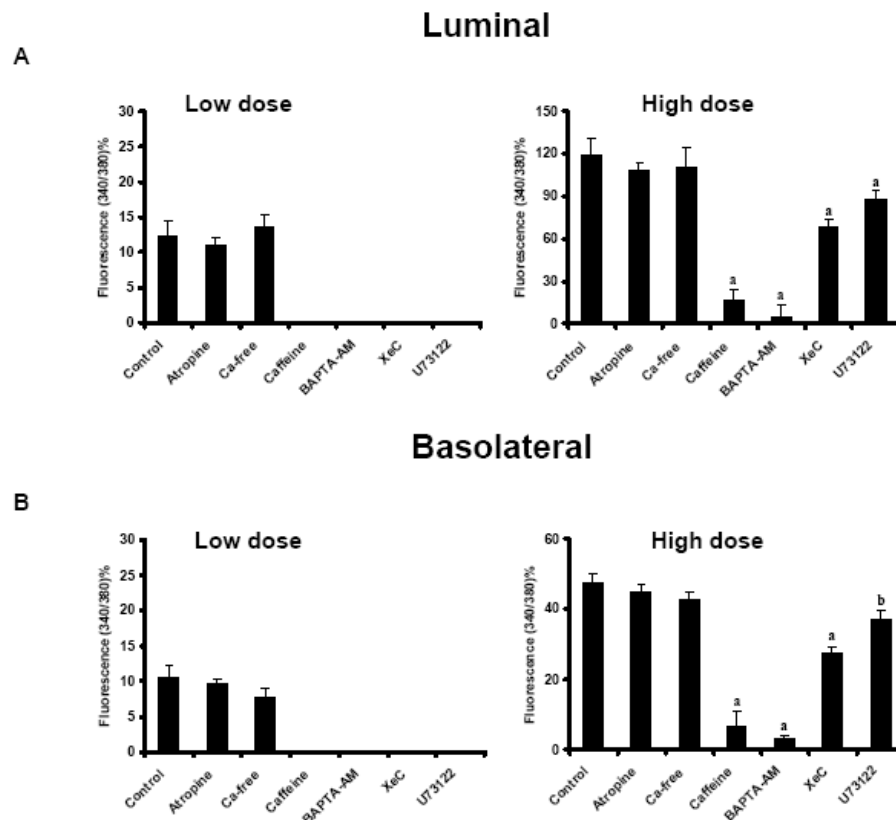


Figure 16. The effect of chenodeoxycholate on $[Ca^{2+}]_i$ under different conditions. Panel A shows the effect of luminal administration of chenodeoxycholate (0.1 and 1 mM). For positive control, 0.1 mM chenodeoxycholate was administered into the lumen. Withdrawal of extracellular calcium and the application of 100 μ M atropine had no effect on chenodeoxycholate -induced Ca^{2+} release. However, preloading the ducts with BAPTA-AM (40 μ M) and caffeine (20 mM) abolished the effect of chenodeoxycholate on $[Ca^{2+}]_i$. **Panel B** shows the effect of basolateral administration of chenodeoxycholate (0.1 and 1 mM). Controls represent response to chenodeoxycholate only. Means and SEM from 25 ROIs of 5 ducts are shown. a: $p < 0.001$ vs. control, b: $p < 0.05$ vs. the control.

4. DISCUSSION

Pancreatitis is the inflammation of the pancreas, which has two main forms: acute and chronic. Acute pancreatitis occurs suddenly and may result in life-threatening complications. The two most frequent etiological factors causing the acute form are blockage of the pancreatic duct by a gallstone or heavy alcohol ingestion. Other causes include hyperlipidemia, hypercalcemia, viral infection, and in a few cases, the disease can have autoimmune or hereditary origin [63]. Chronic pancreatitis is primarily caused by prolonged alcohol ingestion resulting in irreversible damage to the exocrine and endocrine pancreatic tissue. In a small percentage of the cases, especially at patients with young age, who do not consume alcohol, chronic pancreatitis tends to run in their families, suggesting a hereditary background [64].

Development of *in vivo* experimental models of acute pancreatitis has enabled us to study the pathogenesis of the disease [65, 66, 67]. For example, administration of a supramaximally stimulating dose of cholecystokinin analog cerulein to rodents results in either mild (rats) or severe (mice) acute edematous pancreatitis which develops over hours [68, 69]. Other types include L-arginine- or L-ornithine-induced necrotizing [70, 71, 72, 73, 74], bile acid-induced necrotizing and haemorrhagic [75, 76] types. These models are well-characterized in the rat and mouse but, surprisingly, only a few studies were published about experiments on guinea pigs [77, 78, 79].

All species sequenced to date contain multiple trypsinogen genes in their genome, of which only a limited number are expressed at the protein level [80]. In humans, 9 genomic trypsinogen sequences were identified, but only 3 isoforms are expressed to measurable protein levels [2]. The mouse genome contains 20 trypsinogen genes, but the resting mouse pancreas secretes only 4 trypsinogen isoforms (M. Sahin-Toth, unpublished data). The finding that the guinea pig pancreas secretes a single major isoform indicates that multiple isoforms are not an obligatory requirement for digestion, but they probably confer species-specific adaptive advantages. The guinea pig genome has not been sequenced yet, but it is very likely that it also contains multiple trypsinogen genes. This assumption is supported by the cloning of the 2 nearly identical cDNA forms, indicating the presence of at least 2 recently duplicated genes.

Although we posit that the guinea pig pancreas expresses 2 different mRNAs for pre-trypsinogen, which result in the expression of a single mature trypsinogen, there are caveats to this conclusion. First, the biochemical approach utilized here may not detect isoforms present in low quantities (1 % or less of total trypsinogens). Second, the cDNA cloning approach used may not identify isoforms in which the cDNA sequence around the catalytic Ser is less conserved, or isoforms present in very low amounts. Finally, hormonal stimulation of the pancreas may result in the expression of additional trypsinogen isoforms, which have not been found in this study.

Autoactivation of trypsinogen is believed to facilitate physiological zymogen activation in the duodenum. During autoactivation trypsin activates trypsinogen to trypsin, resulting in a self-amplifying reaction. Mutations in the human cationic trypsinogen that cause acceleration of autoactivation *in vitro* have been associated with hereditary pancreatitis, suggesting that autoactivation may be important for premature trypsinogen activation during pancreatitis, at least in humans [81]. The inability of the guinea pig trypsinogen to autoactivate indicates that this mode of trypsinogen activation is not

universally required for digestion. Therefore, the strong tendency for autoactivation observed with the human trypsinogens may indicate a positive evolutionary selection. The relatively high abundance of surface exposed charged side chains (Glu, Asp, Lys, Arg) in the human trypsinogens and their absence in the guinea pig trypsinogen suggests that efficient autoactivation requires interactions associated with these strongly polar amino acids.

There have been only scarce reports on experimental pancreatitis models using the guinea pig and the role of premature trypsinogen activation in the onset of pancreatitis has not been studied in this species. Furthermore, the inability of guinea pig trypsinogen to undergo autoactivation suggests that this species might be more resistant to pancreatitis than humans, where increased autoactivation of cationic trypsinogen mutants has been linked to hereditary pancreatitis.

Research on the pathomechanism of chronic pancreatitis came from relatively recent studies investigating the genes encoding cationic trypsinogen (*PRSS1*), anionic trypsinogen (*PRSS2*), and the pancreatic secretory trypsin inhibitor (*SPINK1*). Gain-of-function variants in cationic trypsinogen have been linked to autosomal dominant hereditary pancreatitis and subsequently also to idiopathic chronic pancreatitis [28, 82, 83, 84]. Recently, triplication of the locus of cationic trypsinogen has been observed in a subset of families with hereditary pancreatitis [85]. *In vitro* biochemical studies revealed that the majority of disease predisposing cationic trypsinogen variants increase autocatalytic conversion of trypsinogen to active trypsin and probably promote premature intrapancreatic trypsin activation *in vivo* [81, 86]. Consistent with the central pathophysiological role of trypsin, p.N34S and other loss-of-function alterations in the trypsin inhibitor *SPINK1* predispose to idiopathic, tropical, and alcoholic chronic pancreatitis [87, 88, 89, 50, 90]. In contrast to pathogenic variations of cationic trypsinogen and pancreatic secretory trypsin inhibitor, the p.G191R variant of the anionic trypsinogen affords protection against chronic pancreatitis due to rapid autodegradation [32]. Taken together, genetic and biochemical evidence defines a pathological pathway in which a sustained imbalance between intrapancreatic trypsinogen activation and trypsin inactivation results in the development of chronic pancreatitis. It has been recently demonstrated that chymotrypsin C degrades all human trypsin and trypsinogen isoforms with high specificity and appears identical to enzyme Y, the enigmatic trypsinogen-degrading activity described by Heinrich Rinderknecht in 1988 [16]. From these studies, chymotrypsin C emerged as a strong novel candidate for a pancreatitis-associated gene.

Here we found that two alterations in the chymotrypsin gene (p.R254W and p.K247_R254del) were significantly overrepresented in all of the pancreatitis groups (idiopathic, hereditary chronic and alcoholic chronic types) compared to controls, in an extensive study, where more than 3700 individuals have been screened. This comprehensive mutation screening of the human chymotrypsin gene reveals the

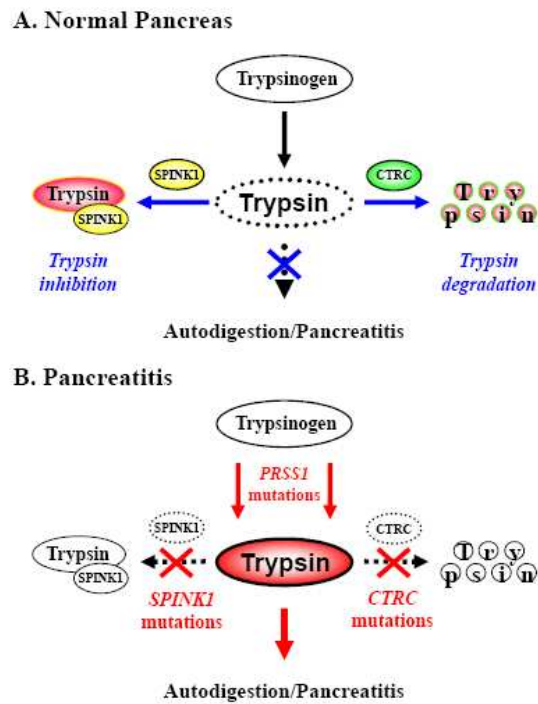


Figure 17. The trypsin dependent pathological model of chronic pancreatitis. Pancreatic defense mechanisms against unwanted trypsin activity include trypsin inhibition by SPINK1 (pancreatic secretory trypsin inhibitor) and trypsin degradation by CTRC. *PRSSI* (cationic trypsinogen) missense variants stimulate activation of trypsinogen to trypsin or block degradation of active trypsin, whereas *SPINK1* alterations reduce inhibitor levels and thus compromise trypsin inhibition. *CTRC* variations abolish activity or decrease secretion of CTRC and thereby impair trypsin degradation.

importance of a possible role of mutations in minor proteases in the initiation of pancreatitis. Furthermore, the investigations of functional consequences of the two chymotrypsin C variants, which showed decreased secretion (R254W) or totally diminished secretion and protease activity (R254del) strengthened our hypothesis about the role of loss-of-function mutations in trypsin-degrading enzymes in increasing the risk for pancreatitis (Fig 17). In summary, the genetic and functional data presented here identify chymotrypsin C as a novel pancreatitis associated gene. Our observations provide further support for the trypsin-dependent pathogenic model of chronic pancreatitis in humans by demonstrating that trypsin/trypsinogen degradation by chymotrypsin C is an important mechanism in the maintenance of the physiological protease-antiprotease balance in the pancreas (Fig 17). These results (while this Nature Genetics paper appeared in print in the

first issue of 2008) have just been confirmed by another study of the human chymotrypsin C, which came out from an independent research group in a lesser journal [91], during the writing of this thesis.

The next challenge was to identify whether bile acids and/or trypsin (e.g. during bile-induced acute pancreatitis) can trigger calcium signalling in guinea pig pancreatic ducts, if so, than we planned to determine the intracellular mechanisms by which chenodeoxycholate stimulates calcium signals. Bile acids induce an elevation in $[Ca^{2+}]_i$ in various cell types including pneumocytes [92], hepatocytes [93], colonocytes [94] gastric mucosal cells [95], vascular endothelial cells [96] and importantly pancreatic acinar cells [35]. The fact that taurodeoxycholic acid-induced DIDS sensitive ^{125}I efflux can be inhibited by BAPTA-AM in dog pancreatic duct epithelial cells suggests that bile acids may induce Ca^{2+} signalling in these cells [97]. In our study we showed, for the first time, that both unconjugated and conjugated bile acids induce a dose-dependent elevation of $[Ca^{2+}]_i$ in guinea pig pancreatic ductal epithelial cells. The unconjugated chenodeoxycholate had significantly larger effects than the conjugated glycochenodeoxycholate. Notably, the effect of luminal administration of a low dose of glycochenodeoxycholate was almost undetectable. We also showed that the Ca^{2+} signal induced by luminal administration of low doses of chenodeoxycholate was totally blocked by the calcium chelator BAPTA-AM, caffeine, the IP_3 receptor inhibitor xestospongine C and the phospholipase C (PLC) inhibitor U73122, but unaffected by removal of extracellular Ca^{2+} . The above mentioned inhibitors also had a similar effect on the $[Ca^{2+}]_i$ elevation evoked by basolateral administration of a high dose of chenodeoxycholate.

PAR-2 has been shown to be expressed in the pancreas [43, 44, 45], therefore, it is possible that activated trypsin (either by autoactivation or as a consequence of the lack of trypsin inhibitor or the trypsin-degrading chymotrypsin C) cleaves PAR-2 and stimulates cellular responses. In our experiments trypsin evoked calcium signalling in pancreatic duct epithelial cells, which proved to be specific responses as PAR-2 activating peptide triggered the same stimulatory effect and the signal could be blocked by a trypsin inhibitor. Trypsin mobilized almost exclusively intracellular calcium stores. PAR-2 expression was also detected by immunostaining of the guinea pig pancreas on the luminal membrane of intralobular ducts. In summary, during pathological conditions, trypsin and bile acids can activate pancreatic ductal epithelial cells through intracellular calcium signalling mechanisms and the activated cells might play an important role during the inflammation of the pancreatic tissue.

5. ACKNOWLEDGEMENTS

I am grateful to **Prof. János Lonovics** and **Prof. Tibor Wittman**, past and present Head of First Department of Medicine, University of Szeged, for providing me with the possibility to do the Ph.D. studies in their department. I express my gratitude to **Prof. Tamás Takács** for giving me the opportunity to join his scientific team. I am also grateful to **Prof. András Varró**, the Head of Department of Pharmacology and Pharmacotherapy, who provided us the opportunity to work in his department .

I am especially thankful to **Dr. Péter Hegyi** and **Dr. Zoltán Rakonczay**, my supervisors, who introduced me into the scientific research of the pancreas, helped and taught me during the experiments. I deeply appreciate the valuable knowledge learnt from them. I am also grateful to **Dr. Miklós Sahin-Tóth** from the Boston University, USA, who introduced me into the biochemical studies of recombinant proteases and to **Dr. Ferenc Rosztoczy**, founder of the Rosztoczy Foundation, who supported me with the Rosztoczy scholarship in Boston. I am really thankful to **Prof. Barry E. Argent** and **Dr. Mike A. Gray** our collaborators from the University of Newcastle, UK for their support and help in our projects.

I would also like to thank my colleagues (**Viktória Venglovecz**, **Dr. Richárd Szmola**, **Dr. Orsolya Király**, **Dr. Edit Szepessy**, **Imre Ignáth**) for their help. I express my gratitude to **Dr. Katalin Borka** (2nd Department of Pathology, Semmelweis University, Budapest), who performed immunostainings for the PAR-2 study.

This work would not have been possible to accomplish without the assistance of **Zoltánné Fuksz**, **Edit Magyariné Pálfi**, **Ágnes Sitkei**, **Vera Sahin-Tóth**, **Miklósné Árva**.

This work was supported by the Hungarian **Scientific Research Fund grants T43066** (János Lonovics) and **PF6395** (Zoltán Rakonczay), **Asboth Grant XTPPSRT1** (János Lonovics), **Bolyai Postdoctoral Fellowship 00276/04** (Péter Hegyi) and **00218/06** (Zoltán Rakonczay), grant from the Royal Society and **KPI Research Grant KPI/BIO-37** (András Varró), by **NIH grant DK058088** (Miklós Sahin-Tóth), a **scholarship from the Rosztoczy Foundation** (to Béla Ózsvári), by the Medical Faculty of the University of Leipzig **formel.1** (to Jonas Rosendahl), the **DFG** (Deutsche Forschungsgemeinschaft) **grant Te 352/2-1** (to Niels Teich) and **grants Wi 2036/2-1 & Wi 2036/2-2** (to Heiko Witt).

My deepest thanks are due to **my family** for their love, support and hard work.

6. REFERENCES

1. Bhatia M, Wong FL, Cao Y, et al. Pathophysiology of Acute Pancreatitis. *Pancreatology* 2005;5:132–144.
2. Chen JM, Férec C. Trypsinogen genes: evolution, In: Cooper DN, Ed. *Nature encyclopedia of the human genome*. London, PA: Macmillan; 2003:645-650.
3. Guy O, Lombardo D, Bartelt A, et al. Two human trypsinogens. Purification, molecular properties, and N-terminal sequences. *Biochemistry* 1978;17:1669–1675.
4. Rinderknecht H, Renner IG, Carmack C. Trypsinogen variants in pancreatic juice of healthy volunteers, chronic alcoholics and patients with pancreatitis and cancer of the pancreas. *Gut* 1979;20:886–891.
5. Rinderknecht H, Stace NH, Renner IG. Effects of chronic alcohol abuse on exocrine pancreatic secretion in man. *Dig Dis Sci* 1985;30:65–71.
6. Rinderknecht H, Renner IG, Abramson SB, et al. Mesotrypsin: a new inhibitor-resistant protease from a zymogen in human pancreatic tissue and fluid. *Gastroenterology* 1984;86:681–692.
7. Nyaruhucha CN, Kito M, Fukuoka SI. Identification and expression of the cDNA-encoding human mesotrypsin (ogen), an isoform of trypsin with inhibitor resistance. *J Biol Chem* 1997;272:10573–10578.
8. Hermon-Taylor J, Perrin J, Grant DAW, et al. Immunofluorescent localisation of enteropeptidase in human small intestine. *Gut* 1977;18:259-265.
9. Kunitz M, Northrop JH. Crystalline chymotrypsin and chymotrypsinogen. I. Isolation, crystallisation and general properties of a new proteolytic enzyme and its precursor. *J Gen Physiol* 1935;18:433-441.
10. Hudaky P, Kaslik Gy, Venekei I, et al.. The differential specificity of chymotrypsin A and B is determined by amino acid 226. *Eur J Biochem* 1999;259:528-533.
11. Bergmann M, Fruton GW. On proteolytic enzymes. XIII. Synthetic substrates for chymotrypsin. *J Biol Chem* 1937;118:405-415.
12. Fruton GW, Bergmann M. The multiple specificity of chymotrypsin. *J Biol Chem* 1942;145:253-265.
13. Brown KD, Shupe RE, Laskowski M. Crystalline activated protein B (chymotrypsin B). *J Biol Chem* 1948;173:99-108.

14. Folk JE, Schirmer WE. Chymotrypsin C. I. Isolation of the zymogen and the active enzyme: preliminary structure and specificity studies. *J Biol Chem* 1965;240:181-192.
15. Nemoda Z, Sahin-Tóth M. Chymotrypsin C (caldecrin) stimulates autoactivation of human cationic trypsinogen. *J Biol Chem* 1996;281:11879–11886.
16. Szmola R, Sahin-Tóth M. Chymotrypsin C (caldecrin) promotes degradation of human cationic trypsin: Identity with Rinderknecht's enzyme Y. *PNAS* 2007;104:11227–11232.
17. Bhatia M, Brady M, Shokuhi S, et al. Inflammatory mediators in acute pancreatitis. *J Pathol* 2000;190:117–125.
18. Bhatia M, Neoptolemos JP, Slavin J. Inflammatory mediators as therapeutic targets in acute pancreatitis. *Curr Opin Investig Drugs* 2001;2:496–501.
19. Bhatia M. Novel therapeutic targets for acute pancreatitis and associated multiple organ dysfunction syndrome. *Curr Drug Targets Inflamm Allergy* 2002;1:343–351.
20. Pandol SJ. Acute pancreatitis. *Curr Opin Gastroenterol* 2006;22:481-486.
21. Thrower EC, Diaz d V, Kolodecik TR, et al. Zymogen activation in a reconstituted pancreatic acinar cell system. *Am J Physiol Gastrointest Liver Physiol* 2006;290:894–902.
22. Figarella C, Miszczuk-Jamska B, Barret AJ. Possible lysosomal activation of pancreatic zymogens: Activation of both human trypsinogens by cathepsin B and spontaneous acid activation of human trypsinogen. *Biol Chem Hoppe-Seyler* 1988;369:293–298.
23. Gorelick FS, Otani T. Mechanisms of intracellular zymogen activation. *Bailliere's Clin Gastroenterol* 1999;13:227–240.
24. Lerch MM, Halangk W, Kruger B. The role of cysteine proteases in intracellular pancreatic serine protease activation. *Adv Exp Med Biol* 2000;477:403–411.
25. Rakonczay Z Jr, Hegyi P, Takács T, et al. The role of NF- κ B activation in the pathogenesis of acute pancreatitis. *Gut* 2008, in press.
26. Naruse S. Molecular pathophysiology of pancreatitis. *Intern Med* 2003;42:288–289.
27. Comfort MW, Steinberg AG. Pedigree of a family with hereditary chronic relapsing pancreatitis. *Gastroenterology* 1952;21:54-63.
28. Whitcomb DC, Gorry MC, Preston RA, et al. Hereditary pancreatitis is caused by a mutation in the cationic trypsinogen gene. *Nat Genet* 1996;14:141-145.
29. Sahin-Tóth M, Tóth M. Gain-of-function mutations associated with hereditary pancreatitis enhance autoactivation of human cationic trypsinogen. *Biochem Biophys Res Commun* 2000;278:286-289.

30. Király O, Guan L, Szepessy E, et al. Expression of human cationic trypsinogen with an authentic N terminus using intein-mediated splicing in aminopeptidase P deficient *Escherichia coli*. *Protein Expr Purif* 2006;48:104-111.
31. Chen JM, Audrezet MP, Mercier B, et al. Exclusion of Anionic Trypsinogen and Mesotrypsinogen Involvement in Hereditary Pancreatitis without Cationic Trypsinogen Gene Mutations. *Scand J Gastroenterol* 1999;34:831-832.
32. Witt H, Sahin-Tóth M, Landt O, et al. A degradation-sensitive anionic trypsinogen (PRSS2) variant protects against chronic pancreatitis. *Nat Genet* 2006;38:668-673.
34. Opie EL. The etiology of acute haemorrhagic pancreatitis. *Johns Hopkins Hospital Bulletin* 1901;12:182-188.
35. Voronina S, Longbotton R, Sutton R, et al. Bile acids induce calcium signals in mouse pancreatic acinar cells: implications for bile-induced pancreatic pathology. *J Physiol* 2002;540:49-55.
36. Raraty M, Ward J, Erdemli G, et al. Calcium-dependent enzyme activation and vacuole formation in the apical granular region of pancreatic acinar cells. *Proc Natl Acad Sci USA* 2000;97:13126-13131.
37. Kim JY, Kim KH, Lee JA, et al. Transporter-mediated bile acid uptake causes Ca^{2+} -dependent cell death in rat pancreatic acinar cells. *Gastroenterology* 2002;122:1941-53.
38. Czako L, Yamamoto M, Otsuki M. Exocrine pancreatic function in rats after acute pancreatitis. *Pancreas* 1997;15:83-90.
39. Hegyi P, Rakonczay Z Jr. The inhibitory pathways of pancreatic ductal bicarbonate secretion. *International Journal of Biochemistry and Cell Biology* 2007;39:25-30.
40. Dery O, Corvera CU, Steinhoff M, et al. Proteinase activated receptors: novel mechanisms of signaling by serine proteases. *Am J Physiol* 1998;274:C1429-1452.
41. D'Andrea RM, Derian KC, Leturcq D, et al. Characterization of protease-activated receptor-2 immunoreactivity in normal human tissues. *J Histochem Cytochem* 1998;46:157-164.
42. Bohm SK, Kong WY, Bromme D, et al. Molecular cloning, expression and potential functions of the human proteinase-activated receptor-2. *Biochem J* 1996;314:1009-1016.
43. Nguyen TD, Moody MW, Steinhoff M, et al. Trypsin activates pancreatic duct epithelial cell ion channels through proteinase-activated receptor-2. *J Clin Invest* 1999;103:261-269.
44. Alvarez C, Regan PJ, Merianos D, et al. Protease-activated receptor-2 regulates bicarbonate secretion by pancreatic duct cells in vitro. *Surgery* 2004;669-676.

45. Namkung W, Han W, Luo X, et al. Protease-activated receptor 2 exerts local protection and mediate some systemic complications in acute pancreatitis. *Gastroenterology* 2004;126:1844-1859.
46. Lengyel Z, Pál G, Sahin-Tóth M. Affinity purification of recombinant trypsinogen using immobilized ecotin. *Protein Expr Purif* 1998;12:291-294.
47. Sahin-Tóth M. Human cationic trypsinogen. Role of Asn-21 in zymogen activation and implications in hereditary pancreatitis. *J Biol Chem* 2000; 275:22750-22755.
48. Szilágyi L, Kénesi E, Katona G, et al. Comparative in vitro studies on native and recombinant human cationic trypsins. Cathepsin B is a possible pathological activator of trypsinogen in pancreatitis. *J Biol Chem* 2001;276:24574-24580.
49. Kukor Z, Tóth M, Sahin-Tóth M. Human anionic trypsinogen. Properties of autocatalytic activation and degradation and implications in pancreatic diseases. *Eur J Biochem* 2003;270:2047-2058.
50. Király O, Wartmann T, Sahin-Tóth M. Missense mutations in pancreatic secretory trypsin inhibitor (SPINK1) cause intracellular retention and degradation. *Gut* 2007;56:1433-1438.
51. Argent BE, Arkle S, Cullen MJ, et al. Morphological, biochemical and secretory studies on rat pancreatic ducts maintained in tissue culture. *Q J Exp Physiol* 1986;71:633-648.
52. Hegyi P, Rakonczay Z Jr, Tizslavicz A, et al. Protein Kinase C modulates the inhibitory effect of substance P. *AJP Cell Physiology* 2005;288:C1030-1041
53. Hegyi P, Gray MA, Argent BE. Inhibitory effect of substance-P on the pancreatic ductal bicarbonate secretion in guinea pig. *Am J Physiol Cell Physiol* 2003;285:268-276.
54. Hegyi P, Rakonczay Z Jr, Gray MA, et al. Measurement of intracellular pH: A new method for analyzing the fluorescence data. *Pancreas* 2004;28:427-434.
55. Hegyi P, Ördög B, Rakonczay Z Jr, et al. The effect of herpesvirus infection on pancreatic duct cell secretion. *World J Gastroenterol* 2005;38:5997-6002.
56. Ishiguro H, Steward MC, Lindsay ARG, et al. Accumulation of intracellular HCO_3^- by $\text{Na}^+\text{-HCO}_3^-$ cotransport in interlobular ducts from guinea-pig pancreas. *J Physiol* 1996;495:169-178.
57. Teich N, Le Maréchal C, Kukor Z, et al. Interaction between trypsinogen isoforms in genetically determined pancreatitis: mutation E79K in cationic trypsin (PRSS1) causes increased transactivation of anionic trypsinogen (PRSS2). *Hum Mutat* 2004;23:22-31.

58. Várallyay E, Pál G, Patthy A, et al. Two mutations in rat trypsin confer resistance against autolysis. *Biochem Biophys Res Commun* 1998;243:56-60.
59. Kukor Z, Tóth M, Pál G, et al. Human cationic trypsinogen. Arg¹¹⁷ is the reactive site of an inhibitory surface loop that controls spontaneous zymogen activation. *J Biol Chem* 2002;277:6111-6117.
60. Mallory PA, Travis J. Human pancreatic enzymes. Characterization of anionic human trypsin. *Biochemistry* 1973;12:2847-2851.
61. Colomb E, Guy O, Deprez P, et al. The two human trypsinogens: catalytic properties of the corresponding trypsins. *Biochim Biophys Acta* 1978;525:186-193.
62. Jessop NW, Hay RJ. Characteristics of two rat pancreatic exocrine cell lines derived from transplantable tumors. *In Vitro* 1980;16:2-12.
63. DiMagno MJ, DiMagno EP. New advances in acute pancreatitis. *Current Opinion in Gastroenterology* 2007;23:494–501.
64. Rosendahl J, Bodeker H, Mossner J, et al. Hereditary chronic pancreatitis. *Orphanet Journal of Rare Diseases* 2007;2:1.
65. Weber CK, Adler G. From acinar cell damage to systemic inflammatory response: Current concepts in pancreatitis. *Pancreatology* 2001;1:356–362.
66. Hegyi P, Takács T, Jármay K, et al. Spontaneous and cholecystokinin-octapeptide-promoted regeneration of the pancreas following L-arginine-induced pancreatitis in rat. *Int J Pancreatol* 1997;22:193-200.
67. Hegyi P, Takács T, Tizslavicz L, et al. Recovery of exocrine pancreas six months following pancreatitis induction with L-arginine in streptozotocin-diabetic rats. *J Physiol Paris* 2000;94:51-55.
68. Lampel M, Kern HF. Acute interstitial pancreatitis in the rat induced by excessive doses of a pancreatic secretagogue. *Virchows Arch A Pathol Anat Histol* 1977;373:97–117.
69. Rakonczay Z Jr, Takács T, Mándi Y, et al.. Water immersion pretreatment decreases pro-inflammatory cytokine production in cholecystokinin-octapeptide-induced acute pancreatitis in rats: possible role of HSP72. *Int J Hyperthermia* 2001;17:520-535.
70. Hegyi P, Rakonczay-Jr Z, Sári R et al. L-arginine induced experimental pancreatitis. *World J Gastroenterol* 2004;10:2003-2009.
71. Hegyi P, Rakonczay Z Jr, Sári R et al. Insulin is necessary for the hypertrophic effect of CCK-8 following acute necrotizing experimental pancreatitis. *World J Gastroenterol* 2004;10:2275-2277.

72. Rakonczay Z Jr, Jármay K, Kaszaki J et al. NF- κ B activation is detrimental in arginine-induced acute pancreatitis. *Free Radical Biol Med* 2003;34:696-709.
73. Hegyi P, Czakó L, Takács T, et al. Pancreatic secretory responses in L-arginine-induced pancreatitis: comparison of diabetic and nondiabetic rats. *Pancreas* 1999;19:167-174.
74. Rakonczay Z Jr, Hegyi P, Dósa S, et al. A new severe acute necrotizing pancreatitis model induced by L-ornithine in rats. *Crit Care Med* 2008 (accepted)
75. Aho HJ, Koskensalo SM, Nevalainen TJ. Experimental pancreatitis in the rat. Sodium taurocholate-induced acute haemorrhagic pancreatitis. *Scand J Gastroenterol* 1980;15:411-416.
76. Rakonczay Z Jr, Takács T, Iványi B, et al. The effects of hypo- and hyperthermic pretreatment on sodium taurocholate-induced acute pancreatitis in rats. *Pancreas* 2002;24:83-89.
77. Harell D, Orda R, Wiznitzer T, et al. Proteolytic proenzymes in the pancreas in the course of experimental bile-induced pancreatitis in the guinea pig. *Digestion* 1978;18:394-401.
78. Frick TW, Hailemariam S, Heitz PU, et al. Acute hypercalcemia induces acinar cell necrosis and intraductal protein precipitation in the pancreas of cats and guinea pigs. *Gastroenterology* 1990;98:1675-1681.
79. Frick TW, Spycher MA, Heitz PU, et al. Ultrastructure of the guinea pig pancreas in acute hypercalcemia. *Pancreas* 1992;7:287-94.
80. Roach JC, Wang K, Gan L, et al. The molecular evolution of the vertebrate trypsinogens. *J Mol Evol* 1997;45:640-652.
81. Teich N, Rosendahl J, Tóth M, et al. Mutations of human cationic trypsinogen (PRSS1) and chronic pancreatitis. *Hum Mutat* 2006;27:721-730.
82. Gorry MC, Gabbazadeh D, Furey W, et al. Mutations in the cationic trypsinogen gene are associated with recurrent acute and chronic pancreatitis. *Gastroenterology* 1997;113:1063-1068.
83. Teich N, Mössner J, Keim V. Mutations of the cationic trypsinogen in hereditary pancreatitis. *Hum. Mutat.* 1998;12:39-43.
84. Witt H, Luck W, Becker M. A signal peptide cleavage site mutation in the cationic trypsinogen gene is strongly associated with chronic pancreatitis. *Gastroenterology* 1999;117:7-10.
85. Le Maréchal C, Masson E, Chen JM, et al. Hereditary pancreatitis caused by

- triplication of the trypsinogen locus. *Nat Genet* 2006;38:1372-1374.
86. Sahin-Tóth M. Biochemical models of hereditary pancreatitis. *Endocrinol Metab Clin North Am* 2006;35:303-312.
87. Witt H, Luck W, Hennies HC, et al. Mutations in the gene encoding the serine protease inhibitor, Kazal type 1 are associated with chronic pancreatitis. *Nat Genet* 2000;25:213-216.
88. Witt H, Luck W, Becker M, et al. Mutation in the SPINK1 trypsin inhibitor gene, alcohol use, and chronic pancreatitis. *JAMA* 2001;285:2716-2717.
89. Bhatia E, Choudhuri G, Sikora SS, et al. Tropical calcific pancreatitis: strong association with SPINK1 trypsin inhibitor mutations. *Gastroenterology* 2002;123:1020-1025.
90. Boulling A, Le Marechal C, Trouve P, et al. Functional analysis of pancreatitis-associated missense mutations in the pancreatic secretory trypsin inhibitor (SPINK1) gene. *Eur J Hum Genet* 2007;15:936-942.
91. Masson E, Chen JM, Scotet V, et al. Association of rare chymotrypsinogen C (CTRC) gene variations in patients with idiopathic chronic pancreatitis. *Hum Genet* 2008;123:83-91.
92. Oelberg DG, Downey SA, Flynn MM. Bile salt-induced intracellular Ca^{++} accumulation in type II pneumocytes. *Lung* 1990;168:297-308.
93. Combettes L, Berthon B, Doucet E, et al. Bile acids mobilise internal Ca^{2+} independently of external Ca^{2+} in rat hepatocytes. *Eur J Biochem* 1990;190:619-623.
94. Devor DC, Sekar MC, Frizzell RA, et al. Taurodeoxycholate activates potassium and chloride conductances via an IP₃-mediated release of calcium from intracellular stores in a colonic cell line (T84). *J Clin Invest* 1993;92:2173-2181.
95. Molloy M, Batzri S, Dziki AJ, et al. Reversibility of deoxycholate-induced cellular hypercalcemia in rabbit gastric mucosal cells. *Surgery* 1996;119:89-97.
96. Nakajima T, Okuda Y, Chisaki K, et al. Bile acids increase intracellular $Ca^{(2+)}$ concentration and nitric oxide production in vascular endothelial cells. *Br J Pharmacol* 2000;130:1457-1467.
97. Okolo C, Wong T, Moody MW, et al. Effect of bile acids on dog pancreatic duct epithelial cell secretion and monolayer resistance. *Am J Physiol* 2002;283:G1042-1050.

7. ANNEX

SUPPLEMENTARY METHODS OF MUTATION SCREENING IN THE HUMAN CHYMOTRYPSINOGEN GENE.

We designed primers complementary to intronic sequences flanking exons 1-8 of *CTRC* based on the published nucleotide sequence (GenBank # NT_004873). The annealing temperatures (T_{ann}) used in the PCR reactions are also indicated in the Table below.

Oligonucleotides used for PCR amplification and sequencing of *CTRC* (Berlin)

PCR primers		T_{ann}
promoter region and exon 1	forward: 5'-CTCATCTCACCTCAGAGCAG-3'	64°C
	reverse: 5'-TAATCTGGGAAAACGCCACC-3'	
exons 2-3	forward: 5'-ACAGGTGTACCGGGCACTCG-3'	64°C
	reverse: 5'-TCACTGCTGGTTCTGGCAC-3'	
exons 4-5	forward: 5'-CAAGGGCGGTGGAAGCTTGG-3'	64°C
	reverse: 5'-ATACCACAGATGTCATCCCC-3'	
exon 6	forward: 5'-TGACCCTCTGGGACCTTGGC-3'	64°C
	reverse: 5'-TGTGGGTTGGCTTCTCAGCC-3'	
exons 7-8	forward: 5'-GCTAGTCTGACACCCAGGG-3'	64°C
	reverse: 5'-GCAGCTTGTGAGATGGAGCG-3'	
Sequencing primers		
promoter region	forward: 5'-GGCTGAGACAGGAGAATCGC-3'	56°C
exon 1	forward: 5'-GTAACCACCCAAGGTCAGGG-3'	56°C
exons 2-3	forward: 5'-GCCAGCCCCAACTCTGTGC-3'	56°C
exon 4	forward: 5'-GCTACACAGCCAGGAGCAGC-3'	56°C
exon 5	forward: 5'-TCCACTCTCACCTCCCTCTG-3'	56°C
exon 6	forward: 5'-ATCTGCTCCCTGAAGGCCTG-3'	56°C
exon 7	forward: 5'-CCCTCACCATGGGCAGGCTG-3'	56°C
exon 7	reverse: 5'-GTGAATGAGTGAGGGGATGG-3'	56°C
exon 8	forward: 5'-CTGAGGGTATGGCCCAGCAG-3'	56°C

Oligonucleotides used for PCR amplification and sequencing of *CTRC* (Leipzig)

PCR primers		T_{ann}
promoter region and exon 1	forward: 5'-CTCATCTCACCTCAGAGCAG-3'	62°C
	reverse: 5'-CTGGTTGGTAGCATCTGAAC-3'	
exons 2-3	forward: 5'-CTTTCCCCGTGGGCTACCA-3'	62°C
	reverse: 5'-GAAGCTGCTCAGAAAAAGCAGAGTA-3'	
exons 4-5	forward: 5'-GGAAGTGTGAGGCACAAGGCTAC-3'	62°C
	reverse: 5'-TAGAGTGTCTGTACATGGT-3'	
exon 6	forward: 5'-CAGCCTGAGCAACAGAGTGA-3'	62°C
	reverse: 5'-CAGTGAAGCCTCTTCTCTGT-3'	
exon 7	forward: 5'-GCCTCCCAGAATAAGGCCAAG-3'	62°C
	reverse: 5'-GCTACTGGAAGCACTCAACCA-3'	
exon 8	forward: 5'-GGACAAGGCTGGCATGTGA-3'	60°C
	reverse: 5'-GGCTCACTAAACACTTCTCA-3'	
Sequencing primers		
promoter region and exon 1	reverse: 5'-CTGGTTGGTAGCATCTGAAC-3'	62°C
exons 2-3	forward: 5'-GTGGGCTACCAGCCCTATTCA-3'	62°C
exon 4	reverse: 5'-GCCTTCCTTGTGGACTTTCCT-3'	64°C
exon 5	forward: 5'-TCCACTCTCACCTCCCTCTG-3'	62°C
exon 6	forward: 5'-TGACCCTCTGGGACCTTGGC-3'	62°C
exon 7	forward: 5'-GCTAGTCTGACACCCAGGG-3'	62°C
exon 8	forward: 5'-AACTGGCTGAGTGGGGTCTC-3'	62°C

After PCR amplification, the entire coding region and the exon-intron transitions were sequenced. In all patients analyzed in Berlin, both strands of exon 7 were sequenced. All mutations were confirmed with a second independent PCR reaction. PCR reactions were performed using slightly different conditions at the two centers. In Leipzig, 0.75 U AmpliTaq Gold polymerase (Applied Biosystems), 450 $\mu\text{mol/L}$ deoxynucleoside triphosphates, and 0.3 $\mu\text{mol/L}$ of each primer were used in a total volume of 25 μL . In Berlin, 0.5 U AmpliTaq Gold polymerase, 400 $\mu\text{mol/L}$ deoxynucleoside triphosphates and 0.1 $\mu\text{mol/L}$ primers were used. Cycle conditions were as follows: initial denaturation for 6 min at 95°C; 40 cycles of 20 s denaturation at 95°C, 40 s annealing (see temperatures in Table above) and 90 s primer extension at 72°C; and a final extension step for 6 min at 72°C. In Berlin, 12 min initial denaturation and 2 min final extension was used. PCR products were digested with shrimp alkaline phosphatase (USB) and exonuclease I (USB). Cycle sequencing was performed using BigDye terminator mix (Applied Biosystems). The reaction products were purified with ethanol precipitation or on a Sephadex G-50 column (Amersham) and loaded onto an ABI 3100-Avant or an ABI 3730 fluorescence sequencer (Applied Biosystems).